

Two Extensions of Active Access-Point Joint Optimization Algorithm for Wireless Local-Area Network

Mousumi Saha, Nobuo Funabiki, Bin Wu, and Pradini Puspitaningayu

Abstract—Nowadays, the *IEEE 802.11 wireless local-area network (WLAN)* is commonly employed as a common Internet communication access medium. In *WLAN*, multiple *access-points (APs)* are usually allocated in a wide network field, which may induce interferences and degrade the performance. On the other hand, a finite number of *partially overlapping channels (POCs)* are obtainable on the commonly used *2.4GHz* band. Therefore, to improve the network performance, it is essential to refine *AP* allocations with *POC* assignment and *AP-host* associations in the network to reduce interference. Previously, we introduced the active *AP* configuration algorithm to optimize the number of active *APs* and host associations, and the *AP* joint optimization algorithm to optimize the transmission power, frequency channel, and *CB* or *non-CB POC* to each *AP*. In this study, we present two extensions to the *AP* joint optimization algorithm to further improve the performance of *WLAN*. In the first extension, we consider the *pre-processing stage*, which identifies the promising *APs* locations to reduce the search space. In the second extension, we propose the *post-processing stage*, which further refines the associations of *AP-host* to enhance the network performance. The proposal's effectiveness is verified through simulations using the *WIMNET* simulator in three network scenarios. The simulation results exhibited that the proposal enhanced the throughput performance by minimizing the interference level compared to the existing algorithms.

Index Terms—*IEEE 802.11n*, access point, host association, *AP* allocation, channel bonding, concurrent communication, network configuration, pre-processing, post-processing.

I. INTRODUCTION

WIRELESS *Local Area Network (WLAN)* has become popular due to easy installation, low costs, and flexibility. *WLANs* have been deployed worldwide to supply internet access in different locations, such as companies, educational institutes, airports, shopping malls, hotels, stations, and *IoT* sector [1][2]. Meanwhile, *WLANs* as a general communication technology, play an important role in various *IoT* scenarios, such as smart homes, automated driving, power grid systems, smart cities, and healthcare [3][4][5][6][7]. Figure 1 shows simple topologies of *WLAN*.

Currently, *IEEE 802.11 WLAN* operates in two unlicensed frequency bands: *2.4GHz* and *5GHz*. The *2.4GHz* band

is typically used in indoor environments because of its vast coverage range and greater penetration capability [8].

In the early *WLAN* standards (*IEEE a/b/g*), the channel bandwidth was fixed at *20 MHz*. In order to obtain higher speeds, *IEEE 802.11n* and the later protocols combine adjacent channels to obtain a higher bandwidth (*40 MHz* or more). This technique is known as channel bonding (*CB*), which enhances data transmission by increasing the sub-carrier numbers in *Orthogonal Frequency Division Multiplexing (OFDM)*. For instance, a *20 MHz non-CB* channel uses 52 sub-carriers, while a *40 MHz CB* channel expands this to 114 sub-carriers [9]. *OFDM* utilizes multiple narrow-band carriers to achieve greater linkspeed in *wide-band CB* configurations. However, the use of *CB* can exacerbate *partially overlapping channels (POCs)* due to restricted channel constraints, as shown in Figures 2 (a) and (b).

In *WLAN*, the user distribution is commonly non-uniform [10], and the coverage range of one *AP* is limited due to the *license-free band*. Therefore, to ensure the seamless internet connections, allocating multiple *APs* in a wide area is common. Under the limited available channels, such crowded *APs* often interfere with one another and will degrade network performance due to the overlap of the same frequency signals between them [11].

Meanwhile, higher transmission power, while useful in increasing speed, also boosts interference with other devices in the environment. Therefore, it is necessary to enhance the performance of the *WLAN* under interference by rationally allocating the transmission power, frequency channel, channel bonding, and host association for each *access point*.

To address the above-mentioned issues, we have investigated the elastic *WLAN* system [12][13][14][15]. At the same time, the algorithm based on *local search method* in [12][13], has been introduced to the minimum the number of activated *APs*, host associations, and optimized orthogonal channels. However, this algorithm does not consider the locations of *APs*, it can lead to interference and degrade network performance. Therefore, in [14], we have explored the *pre-processing stage* of the active *AP* configuration algorithm for finding the promising *AP* locations from candidates to enhance the solution quality by reducing the search space of the algorithm.

However, faced with actual scenarios, we found that the algorithm in [14] lacks consideration of concurrent communication. Also, it may not optimize the optimal solution of power. Therefore, to enhance the network performance of *WLAN* under concurrent communication, we have studied the *throughput drop estimation model* in appendix A under the coexistences of *CB* and *non-CB* channels for *concurrently*

Manuscript received May 4, 2024; revised January 26, 2025.

M. Saha is a PhD student of the Department of Information and Communication Systems, Okayama University, Okayama, Japan. (email: sahamousumi@s.okayama-u.ac.jp).

N. Funabiki is a professor of the Department of Information and Communication Systems, Okayama University, Okayama, Japan. (email: funabiki@okayama-u.ac.jp).

B. Wu is a postgraduate student of the Department of Information and Communication Systems, Okayama University, Okayama, Japan. (email: ppxf92cc@s.okayama-u.ac.jp).

P. Puspitaningayu is a lecturer in Universitas Negeri Surabaya, Indonesia. (email: pradinip@unesa.ac.id).

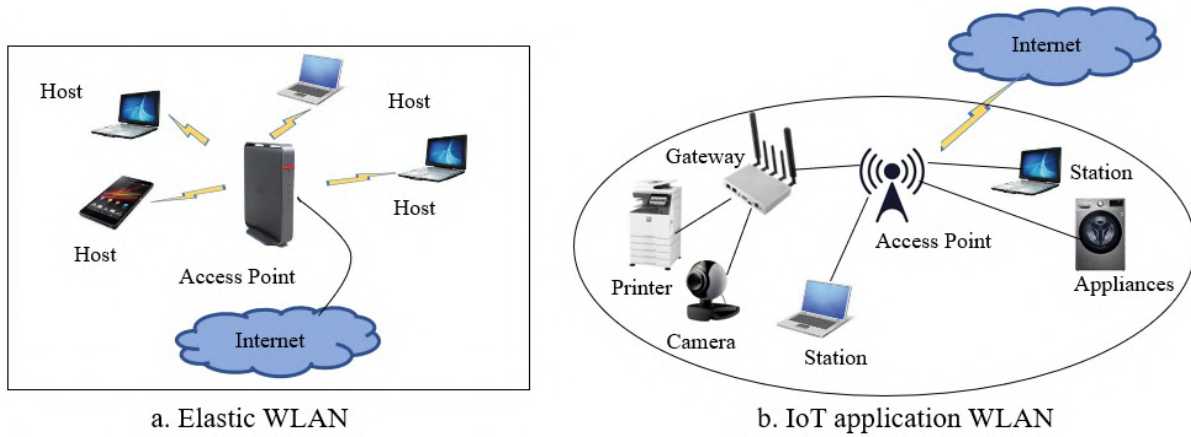
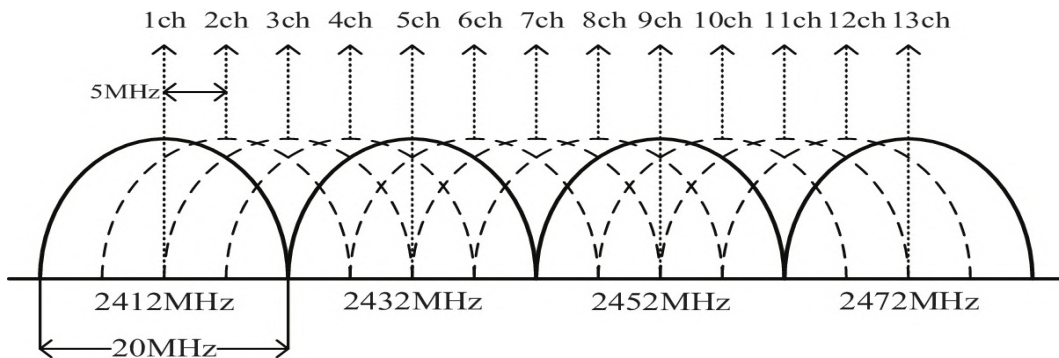
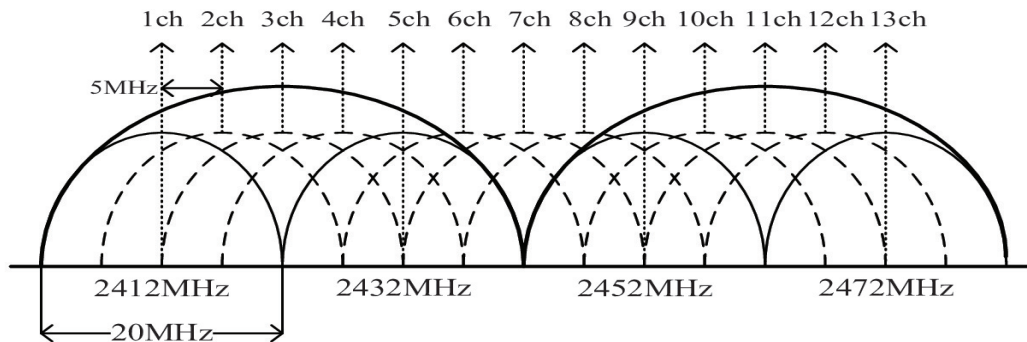


Fig. 1: Overview of WLAN.



(a) 20 MHz POCs.



(b) 40 MHz POCs.

Fig. 2: Non-bonding and bonding channels at 2.4GHz.

communicating links, and proposed the *AP joint optimization algorithm* that jointly optimizes the transmission power, the frequency channel, and the channel bonding (CB) or non-CB to each AP in *IEEE 802.11n WLAN* using the *throughput drop estimation model* [15]. However, since multiple hosts frequently connect to a single AP in real networks, this algorithm only considers a single host association with each AP, which is unrealistic. Furthermore, the active AP configuration algorithm [12] and the *AP joint optimization algorithm* [15], are the *NP-complete* problem that needs extensive computations to get the optimal solution.

Therefore, it is necessary to improve the *AP joint optimization algorithm* to address all of the issues and improve *WLAN* performance [15]. However, optimizing the near-optimal solution into a single algorithm that addresses all issues is challenging due to the larger search space and

huge computations. To address this issue, we sequentially run the active AP configuration algorithm [12] and the *AP joint optimization algorithm* [15]. We observed that some hosts suffered from extremely low throughput due to improper allocation of APs.

To address all these issues, in this study, we present two extensions to the *AP joint optimization algorithm* to improve the performance of *WLAN* networks. In the first extension, we adopt the *pre-processing stage* of the active AP configuration in the *AP joint optimization algorithm* to select the promising candidate APs. This stage not only improves the network performance but also reduces the search space of the network field.

In the second extension, we propose the *post-processing stage* of the algorithm, which refines *AP-host* associations to further enhance the overall network performance.

The effectiveness is assessed through simulations in different network topologies using the *WIMNET simulator* [16]. The results showed that the proposal improved the throughput performance by reducing the interference level compared to the existing methods.

The remaining part of this paper is structured as follows: Section II describes related works. Section III and Section IV review the AP joint optimization algorithm and the pre-processing stage. Section V presents the two extensions of the AP joint optimization algorithm. Section VI evaluates the proposal through simulations. Finally, Section VII concludes this paper with some future directions.

II. REVIEW OF LITERATURE

In this section, we introduce related works in literature. Several studies have addressed various approaches to improve the throughput quality of WLANs.

In [17], Lee et al. introduced a heuristic AP assignment approach for wireless communication in industrial environments. They aimed to decrease the APs number while providing every mobile user with at least two concurrent links with different APs. Their scheme relied on direct measurement of signal strength and used passive repeaters to improve communication reliability. The authors demonstrated the effectiveness and feasibility of their approach through experiments and simulations. Denoting, to this study, we can highlight the significance of concurrent communication and AP location optimization for improving WLAN performance.

In [18], Khattak et al. discussed the challenges of using WLAN fingerprinting for indoor localization in smart and sustainable cities due to limited non-overlapping channels in WLAN networks that cause interference. To address this, they proposed a channel assignment strategy based on the hearability and mutual distance of the APs. They present a simulation model, which demonstrates that the proposed strategy reduces interference among neighboring APs. Denoting, to this study, we can highlight the significance of considering channel interference, channel assignment, and AP location optimization for improving WLAN performance.

In [19], Garroppo et al. presented energy conservation in enterprise WLANs during off-peak hours without compromising coverage and quality of service. The method involves three strategies: AP Management, Device Association, and Power Adjustment. The approach includes creating a comprehensive WLAN model and solving a mathematical problem using a developed algorithm. The aim is to save energy while maintaining WLAN performance. By denoting to this study, we can highlight the significance of improving WLAN performance for high-quality and reliable Internet access.

In [20], Ali et al. proposed a model to detect the best locations of outdoor APs in a large university campus with limited resources. They collected data on the current locations of 17 outdoor access points, 25 demand points, and 14 new potential locations. The Set-Covering model suggests that 21 access points are required to cover all the demand points, while the *maximal-coverage location problem (MCLP)* model shows that 17 access points can cover 92.34% of the demand. By denoting to this study, we can highlight the significance of optimizing the location of WLAN access points for reliable Internet access.

In [21], Liu et al. proposed a method to optimize APs in WLANs and used *Fruit Fly Optimization Algorithm (FOA)* to jointly optimize the location and power of each AP, reducing power consumption and improving coverage rate. Redundant APs were removed below a threshold. However, interference with concurrent communication was not considered.

In [22], Roy et al. proposed an algorithm for dual interfaces with channel bonding that optimizes network performance and reduces the active APs number in dense WLAN environments. The algorithm uses a throughput estimation model, a greedy algorithm, a local search method, and a simulated annealing technique. The proposal was evaluated through simulations and experiments utilizing Raspberry Pi APs and Linux PCs with positive results. However, AP location optimization and power were not considered.

In [23], Tewari et al. presented a joint *power* and *POC* optimization method to enhance the performance of the crowded WLAN network. Efficient use of POC can increase the frequency reuse by reducing the interference range. However, the extreme use of POCs can lead to adjacent channel interferences. To improve the quality of service they proposed an effective power control method, where the effectiveness is confirmed by simulations and does not consider the AP locations.

In [24], Kachroo et al. introduced an algorithm designed to manage both channel and transmission power within a multi-rate WLAN framework operating on standard *20MHz non-CB POC channels*. The process begins with fixed transmission power, during which channels are allocated to APs. Subsequently, the algorithm adjusts transmission power incrementally, either increasing or decreasing it, to optimize the *signal-to-interference-plus-noise ratio (SINR)*. It should be highlighted that their approach does not address the issue of associating hosts with APs. In contrast, our method incorporates host-to-AP associations into the optimization, also taking into consideration the spatial distribution of APs.

In [11], Mittal et al. presented a game theoretic method to balance the APs load. Hosts connected to heavily congested APs are transferred to lower crowded APs to improve link speed. However, concurrent communication interference was not considered.

In [25], Shindo et al. introduced an approach for aggregating *virtual access points (VAPs)* by leveraging two key metrics: the *received signal strength indicator (RSSI)* and the *bandwidth (BW)* consumption. This strategy aims to enhance the throughput for mobile nodes, which can often be impacted negatively by the aggregation of VAPs, while simultaneously reducing the number of APs that remain active. However, their method does not take into account the joint optimization required to handle concurrent communication effectively.

In [26], Yang et al. proposed a selection method to optimize the measurement points for access point (AP) localization to reduce manual efforts and improve accuracy. In their proposal, the next measurement point is determined based on real-time data and is located at the intersection of the coverage areas of APs, whose locations are roughly estimated from previous measurements.

In [27], Kobayashi et al. addressed the issue of optimizing Wi-Fi APs by considering the type and volume of traffic generated by users, rather than assuming a fixed AP position.

The authors proposed *CHASA*, a system that dynamically updates the optimal position of a movable AP based on the type of traffic. This system used a decision tree for traffic classifications and a hill climbing method to find the optimal AP position.

In [28], Alakhras et al. proposed a two-step algorithm for resource allocations in wireless networks, focusing on subcarrier allocations based on channel quality and multicast service priority, followed by power reallocation to enhance system capacity while ensuring QoS. The interval-based algorithm allocates subcarriers and power to multicast groups, aiming to maximize throughput and minimize complexity.

In [29], Mestre et al. proposed an algorithm that chooses the best AP considering the network delay rather than RSSI. The proposal enhanced the overall network performance by choosing APs with the lower delay.

In [30], Deng et al. optimized the layout of WLAN APs to improve location reliability and accuracy by adding minimally redundant APs. They proposed a method to ensure that even if one AP fails, the remaining APs can still cover all the areas with minimal location error.

III. REVIEW OF AP JOINT OPTIMIZATION ALGORITHM

This section review the *AP* joint optimization algorithm for *WLAN*.

A. Elastic WLAN System

In order to realize the optimal configuration of the network, we designed the *elastic WLAN system* to control all the devices in the network through a server to manage the administrative access rights, and the APs use software-based adjustable configuration devices to adopt the optimal configuration through the server's recommendations. With the *elastic WLAN system*, it is possible to dynamically manage the connections between activated APs and hosts depend on the output of the *active AP configuration*.

B. Formulation of Active AP Configuration

The active AP configuration algorithm is formulated as follows in Figure 3:

C. Active AP Configuration Algorithm Description

Figure 4 and 5 illustrates the flow chart and steps for the algorithm of active AP configuration respectively [12][13].

D. Formulation of AP Joint Optimization Algorithm

The AP joint optimization considering the *throughput drop model* in appendix A is formulated as follows in Figure 6 [15].

E. Procedure of Joint Optimization Algorithm

The joint optimization procedure is described in Figure 7.

The maximum transmission power for *CB* and *non-CB* channels is $-20dB$ and $-28.2dB$, respectively, and the minimum for both is $-33.2dB$.

IV. REVIEW OF PRE-PROCESSING STAGE

In this section, we review the *pre-processing stage* of the *active AP configuration algorithm* [14]. For this stage, the exhaustive search approach and the heuristic search approach were proposed.

Figure 8 demonstrates the flow chart for the pre-processing stage. Figure 8 (a) illustrates the exhaustive approach and Figures 8 (b) illustrates the heuristic approach of the pre-processing stage.

A. Formulation of Pre-processing Stage

The pre-processing stage is formulated as follows:

1) Inputs:

- Locations of M candidate APs
- Locations of H hosts
- Locations of walls
- Number of selected APs, N ($N \leq M$)

2) Outputs:

- N promising locations of candidate APs

3) Objectives:

- Maximize the summation of the bottleneck host throughputs for N APs: E
- Maintaining the initial objective, to maximize E_2

B. Exhaustive Search

The exhaustive search approach illustrates in Figure 9:

C. Heuristic Search

The heuristic search approach illustrates in Figure 10:

V. PROPOSAL OF TWO EXTENSIONS OF AP JOINT OPTIMIZATION ALGORITHM

In this section, we present the two extensions of the *AP* joint optimization algorithm. Figure 11 shows the overall execution flow for the two extensions of the *AP* joint optimization algorithm. Figure 11 (a) illustrates the first extension of the *AP* joint optimization algorithm and Figures 11 (b) illustrates the second extension of the *AP* joint optimization algorithm.

A. Formulation of Extended Algorithm

This extended algorithm is formulated as follows:

1) Inputs:

- Locations of M candidate APs
- Locations of H hosts
- Locations of walls

2) Outputs:

- Active APs set
- Set of hosts associated with each active AP
- CB or non-CB POC for each AP
- Maximum or minimum transmission power for each AP

3) Objectives:

- To maximize E_T . E_T is the total throughput of the WLAN network, which is calculated by the sum of the throughputs of all the active APs and their associated hosts

1. **Inputs:**

- Number of hosts: H
- Number of APs: $N = N^D + N^V + N^M$ where N^D , N^V , and N^M represent the number of DAPs, VAPs, and MAPs respectively.
- Link speed between AP_i and $host_j$ for $i = 1$ to N , $j = 1$ to H : tp_{ij} , where the link speed can be estimated by the model in [31].
- Minimum link speed for association: S

2. **Outputs:**

- Set of active APs
- Set of hosts associated with each active AP

3. **Objectives:**

- To minimize E_1
- Holding the first objective, to maximize E_2

E_1 represents the number of active APs (DAPs, VAPs, and MAPs) in the network:

$$E_1 = E_1^D + E_1^V + E_1^M \tag{1}$$

where E_1^D represents the number of active DAPs, E_1^V does the number of active VAPs, and E_1^M does the number of active MAPs respectively.

E_2 indicates the *minimum average host throughput* for the bottleneck AP:

$$E_2 = \min_j [TP_j] \tag{2}$$

where TP_j represents the average host throughput for AP_j that is given by:

$$TP_j = \frac{1}{\sum_k \frac{1}{tp_{jk}}} \tag{3}$$

where tp_{jk} represents the link speed between $node_j$ and $node_k$ ($link_{jk}$).

4. **Constraints:**

- Minimum host throughput constraint: each host in the network must enjoy the given threshold G on average when all the hosts are communicating simultaneously.
- Bandwidth limit constraint: the bandwidth of the wired network to the Internet must be less than or equal to the total available bandwidth of the network B^a .

Fig. 3: Active AP configuration formulation.

• Maintaining the first objective, to maximize E_2
 E_2 describes the *minimum average host throughput* for the bottleneck AP:

$$E_2 = \min_j [TP_j] \tag{1}$$

where TP_j describes the average host throughput for AP_j that is given by:

$$TP_j = \frac{1}{\sum_k \frac{1}{tp_{jk}}} \tag{2}$$

where tp_{jk} describes the link speed between $node_j$ and $node_k$ ($link_{jk}$).

- b) Bandwidth limit constraint: the bandwidth of the wired network to the Internet must be lower than or equal to the total available bandwidth of the network B^a .
- c) Transmission power constraint: the transmission power of each AP must be within a predefined maximum or minimum range.
- d) Frequency channel constraint: the frequency channel of each AP must be one of the available channels at 2.4GHz band.
- e) Channel bonding constraint: the channel bonding of each AP must be either 20MHz or 40MHz.

4) **Constraints:**

- a) Minimum host throughput constraint: all of the simultaneous communicating hosts in the network must have the given threshold G .

B. *First Extension: Pre-processing Stage*

The procedure of the network configuration considering the pre-processing stage of the active AP configuration in the AP joint optimization algorithm is given as follows:

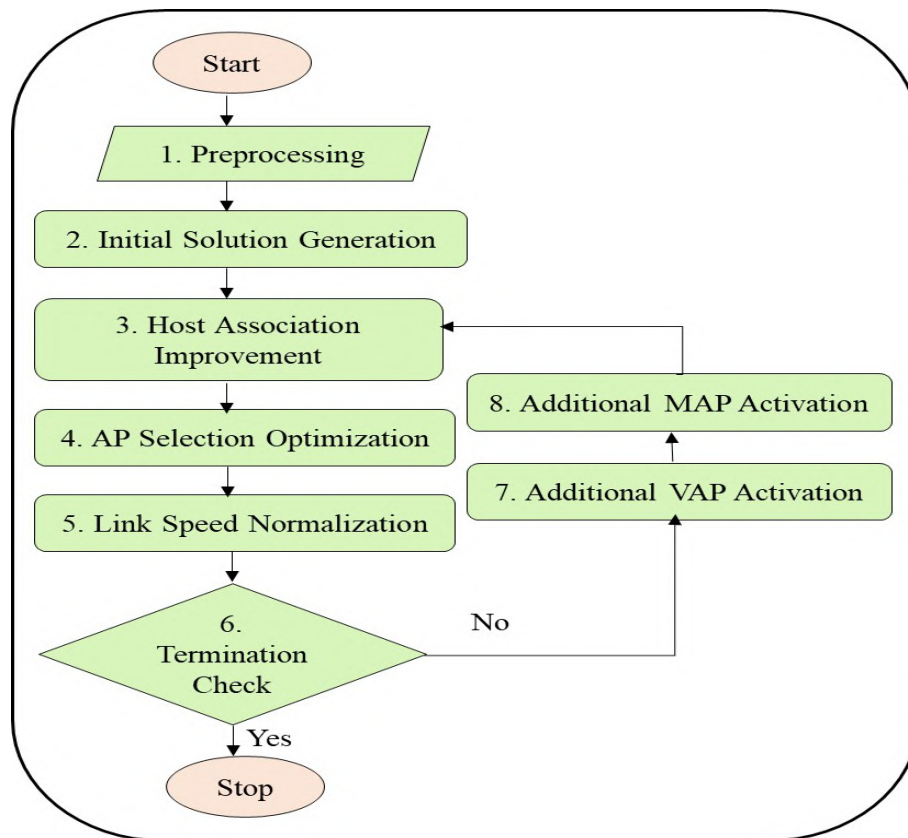


Fig. 4: Flowchart of AP configuration algorithm.

- 1) We select the promising candidate APs at the pre-processing stage. Here, we only consider the exhaustive search approach in Section IV-B.
- 2) We optimize the AP and host associations by the algorithm in Section III-C and optimize the channel, channel type and power of each AP by the algorithm in Section III-E.

C. Second Extension: Post-processing Stage

In the second extension, we present the post-processing stage of the AP joint optimization algorithm.

1) *Post-processing Stage of AP Joint Optimization Algorithm*: The active AP configuration algorithm include the following eight steps in Section III-C. In this paper, we present a new Step 9, namely, *Post Host Association Optimization*, as the post-processing stage. The procedure of the post host association optimization is given as follows:

- 1) Choose one host from the current active host list.
- 2) Randomly select another host whose associated AP is different from the first one.
 - a) Calculate the cost function (G) for the current association.
 - b) Exchange the associations of the two hosts if the cost function is improved. Otherwise, go back to the previous association.
- 3) Repeat Step 2 until all hosts are checked.
- 4) Terminate the algorithm if all active hosts are checked otherwise go back to Step 1.

VI. EVALUATION BY SIMULATIONS

In this section, we evaluate the proposed two extensions of the AP joint optimization algorithm through simulations

using the *WIMNET* simulator [16].

A. Simulation Platform

Figure 12 shows the adopted hardware and software specifications of the *PC* to evaluate the proposal in the simulations.

B. Random Topology

Firstly, the proposal is assessed by adopting a simple network field where *APs* and hosts are randomly allocated in one room.

1) *Random Topology*: Figure 13 (a) demonstrates this random topology. 15 hosts and 15 *APs* are allocated in one $50\text{m} \times 50\text{m}$ room. The circle describes the *AP* and the square does the host. Figures 13 (b) suggests the output of the pre-processing stage.

2) *Results of First Extension*: Figure 14 and Table I demonstrate the first extension results and the simulation results respectively. Figure 14 shows the number of active *APs*, *CB* or *non-CB POC* for each *AP*, and the maximum or minimum transmission power for each *AP* for different value of G . Table I shows the minimum host throughput, the average minimum host throughput, the average host throughput, the average maximum host throughput, and the total throughput respectively. From the simulation results, by the *pre-processing stage* in the first extension, the throughput performance is improved compared to the original method. However, due to the 1 or 2 host associations, in a few cases, some results for $G = 10$ and for $G = 20$ gives lower throughput than the original method.

1. **Preprocessing:** The link speed for any possible pair of an AP and a host is estimated using the throughput estimation model [31].
2. **Initial Solution Generation:** An initial solution is derived using a greedy method [32] of selecting the active APs and host associations that can cover the largest number of hosts. Then, the number of active APs is represented by E_1 .
3. **Host Association Improvement:** The average host throughput E_2 is calculated for the initial solution by:

$$E_2 = \min_j [TP_j] \quad (4)$$

where TP_j represents the average host throughput for the j th AP and is defined by:

$$TP_j = \frac{1}{\sum_k \frac{1}{tp_{jk}}} \quad (5)$$

where tp_{jk} represents the link speed between the j th AP and the k th host. Then, this solution is improved by finding better host associations.

4. **AP Selection Optimization:** E_1 and E_2 are jointly optimized by applying a local search method [33] of randomly changing active APs and finding host associations to minimize them.
5. **Link Speed Normalization:** The fairness criterion is applied here in adjusting the link speed, when the total expected bandwidth B^e exceeds the given total bandwidth B^a :
 - (a) Calculate B^e by taking the summation of the throughputs of all the APs.
 - (b) If $B^e > B^a$, adjust each AP-host link speed as:

$$\hat{t}_{ij} = tp_{ij} \times \frac{B^a}{B^e} \quad (6)$$

where \hat{t}_{ij} is the adjusted link speed, which will be used in the following steps.

6. **Termination Check:** When the *minimum host throughput constraint* is satisfied or all the APs in the network have been activated, go to the next step. Otherwise, go to step 3.
7. **Additional VAP Activation:** If VAPs are not selected for candidate APs, they are newly selected as candidate APs. The locations of hosts are considered as the locations of the candidate VAPs. Then return to step 4.
8. **Additional MAP Activation:** If MAPs are not selected for candidate APs, they are newly selected as candidate APs. The locations of hosts are considered as the locations of the candidate MAPs. Then return to step 4.

Fig. 5: Steps of AP configuration algorithm.

TABLE I: First extension simulation results for random topology.

G mbps	Method	Min. h. thru.	Ave. Min. h thru.	Ave. h. thru.	Ave. Max. h. thru.	Total thru.
10	Original	2.27	2.59	3.39	4.09	50.87
	Only pre.	2.27	2.55	3.33	4.09	49.86
20	Original	3.86	4.32	6.49	8.23	97.44
	Only pre.	2.96	4.71	6.71	7.88	100.68
30	Original	3.25	6.75	8.61	10.57	129.14
	Only pre.	5.81	9.73	11.06	13.29	165.84
35	Original	4.42	10.06	11.53	13.16	173.01
	Only pre.	7.26	10.32	12.38	13.88	185.73

TABLE II: Second extension simulation results for random topology.

G mbps	Method	Min. h. thru.	Ave. Min. h thru.	Ave. h. thru.	Ave. Max. h. thru.	Total thru.
10	Original	2.27	2.59	3.39	4.09	50.87
	With pre. & post.	2.30	2.7	3.93	4.09	50.87
20	Original	3.86	4.32	6.49	8.23	97.44
	With pre. & post.	3.01	5.47	7.14	7.87	107.04
30	Original	3.25	6.75	8.61	10.57	129.14
	With pre. & post.	5.81	9.73	12.01	13.29	165.84
35	Original	4.42	10.06	11.53	13.16	173.01
	With pre. & post.	7.26	10.32	12.38	13.91	185.73

3) *Results of Second Extension:* Figure 15 and Table II show the second extension results and the simulation results respectively. By considering both the *pre-processing* and *post-processing stages* in the second extension, the throughput performance is improved for all cases compared to the original method.

As shown in Table I, the first extension results show that in some cases, such as $G = 20$, there is the lower throughput compared to the original method. However, after the second extension, improvements can be seen in Table II.

To assess the effectiveness of the second extension, we compare the pre-processing and post-processing results for

1. Input and Output: In the algorithm input, the number of channels C_{CB} for *CB POCs* and C_{non} for *non-CB POCs*, and the center frequency of each channel are given.

In the algorithm output, the *CB* or *non-CB POC*, and the *maximum* or *minimum* transmission power is assigned to each active AP, instead of *non-CB, orthogonal channels (OC)*, and the *maximum* transmission power.

2. Objective: In the algorithm objective, the cost function E_{ch} in Eq. (1) maximize the total throughput of the links in WLAN.

$$E_{ch} = \sum_{i=1}^N TP_i^{POC} \quad (1)$$

where TP_i^{POC} represents the total throughput of the links associated with AP_i and N is total number of APs. TP_i^{POC} is calculated by:

$$TP_i^{poc} = \sum_j^m (tp_{ij}^{poc} \times Srf(m)) \quad (2)$$

where m represents the number of hosts associated with AP_i , tp_{ij}^{POC} does the estimated throughput of the link between AP_i and $host_j$ by the proposed model, and $Srf(m)$ does the contention factor at AP_i for associated hosts to send data through CSMA/CA. $Srf(m)$ is calculated by:

$$Srf(m) = \left(\frac{1}{m + \frac{0.1(m-1)}{4}} \right) \times 1 - (0.1 \times m - 1). \quad (3)$$

The constants in Eq. (3) are obtained from measurements by increasing the number of associated hosts to a single AP one by one under no interference.

Fig. 6: Formulation of AP joint optimization algorithm.

$G = 20$. Figure 16 illustrates the random network topology with the AP host associations for $G = 20$. In Figure 16 (a), only the pre-processing is considered, showing that a few hosts suffer from poor associations, leading to the lower throughput and the network performance degradation, as represented by the red marks. In Figure 16 (b), the second extension is illustrated, showing improved associations by refining *AP-host* associations, leading to the overall network performance improvement.

C. Regular Topology 1

Secondly, we assess our proposal adopting a three room regular network field.

1) *Regular Topology 1*: Figure 17 (a) illustrates the regular topology with three rooms, where 20 hosts and 20 APs are regularly allocated in two $20\text{m} \times 30\text{m}$ rooms, one $10\text{m} \times 30\text{m}$ room. Figures 17 (b) suggests the output of the pre-processing stage.

2) *Results of First Extension*: Figure 18 and Table III show the first extension results and the simulation results respectively. Figure 18 shows the number of active APs, *CB* or *non-CB POC* for each AP, and the maximum or minimum transmission power for each AP for different value of G . Table III shows the minimum host throughput, the average minimum host throughput, the average host throughput, the average maximum host throughput, and the total throughput respectively. By considering the *pre-processing stage* in the first extension, the throughput performance is improved compared to the original method.

TABLE III: First extension simulation results for regular topology 1.

G mbps	Method	Min. h. throu.	Ave. Min. h throu.	Ave. h. throu.	Ave. Max. h. throu.	Total throu.
5	Original	0.58	0.72	0.96	1.11	19.25
	Only pre.	0.69	0.82	1.07	1.25	21.53
10	Original	3.6	5.49	7.43	9.22	148.71
	Only pre.	4.98	5.98	7.58	9.19	151.70
15	Original	1.29	7.72	10.26	12.26	205.36
	Only pre.	6.22	10.45	12.26	14.27	245.21
20	Original	7.03	11.49	12.76	14.09	255.20
	Only pre.	5.09	15.07	15.33	17.97	306.73

3) *Results of Second Extension*: Figure 19 and Table IV show the second extension results and the simulation results respectively. By considering both the *pre-processing* and *post-processing stages* in the second extension, the throughput performance is improved for all cases compared to the original method.

After implementing the second extension, significant throughput improvements are observed in most cases in Table IV when compared to the results from the first extension in Table III. To evaluate the effectiveness of the second extension, we compare the *pre-processing and post-processing* results for $G = 15$. Figure 20 depicts the regular network topology with AP host associations for $G = 15$. In Figure 20 (a), only the pre-processing is considered, revealing that a few hosts experience poor associations, resulting in the lower throughput and the network performance degradation, indicated by the red marks. In Figure 20 (b), the second extension is illustrated, demonstrating improved associations

Initially, only *CB* channels with *maximum transmission power* are assigned by the greedy procedure, since they can maximize the throughput in general. Then, this assignment is improved by optimizing the selection of *CB*, *non-CB*, the maximum power, and the minimum power by the following steps [15]:

1. Randomly select one AP with the maximum transmission power for the change trial.
2. Randomly select a different *CB* channel from the current one to this selected AP.
3. Run the throughput estimation model. If the estimated throughput improves E_{ch} in Figure 4, this channel change is accepted. To avoid the local optimum, the hill-climbing procedure is applied where if 0-1 random number is smaller than $\exp(\Delta E_{ch}/Temp)$, where ΔE_{ch} is difference between old and new E_{ch} and $Temp$ is given algorithm parameter for temperature, this channel change is accepted.
4. Go back to Step 1, when the new channel is accepted. Otherwise, go to the next step.
5. Change the transmission power to the minimum and run Step 3.
6. Go back to Step 1, when the new power is accepted. Otherwise, go to the next step.
7. Change the selected channel to *non-CB* and run Step 3.
8. Go back to Step 1, when the new *non-CB* is accepted. Otherwise, go to the next step.
9. Change the transmission power to the maximum and run Step 3.
10. Go back to Step 1.

Fig. 7: Procedure of joint optimization algorithm.

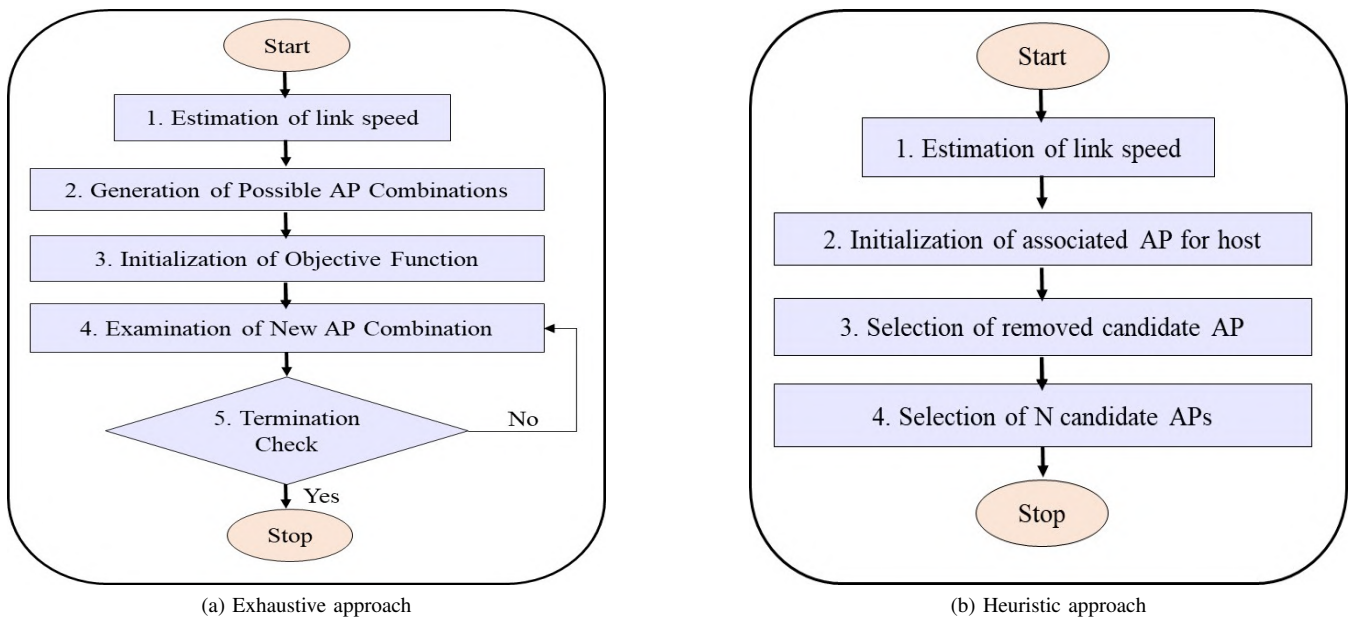


Fig. 8: Flow chart of preprocessing stage.

TABLE IV: Second extension simulation results for regular topology 1.

G Mbps	Method	Min. h. throu.	Ave. Min. h throu.	Ave. h. throu.	Ave. Max. h. throu.	Total throu.
5	Original	0.58	0.72	0.96	1.11	19.25
	With pre. & post.	0.69	0.82	1.07	1.25	21.53
10	Original	3.6	5.49	7.43	9.22	148.71
	With pre. & post.	4.98	5.98	7.58	9.19	151.7
15	Original	1.29	7.72	10.26	12.26	205.36
	With pre. & post.	4.07	8.33	12.54	15.18	250.90
20	Original	7.03	11.49	12.76	14.09	255.20
	With pre. & post.	8.61	15.67	15.81	18.26	316.12

through refining *AP-host associations*, which leads to overall improvements in the network performance.

D. Regular Topology 2

Finally, the proposal is assessed by adopting a five room regular network topology.

1) *Regular Topology 2*: Figure 21 (a) illustrates the regular topology 2 with five rooms, where 30 hosts and 25 APs are regularly allocated in two $20m \times 50m$ rooms, two $10m \times 50m$ rooms, and one $40m \times 50m$ room. Figures 21 (b) suggests the output of the pre-processing stage.

2) *Results of First Extension*: Figure 22 and Table V show the first extension results and the simulation results

1. **Estimation of link speed:** The link speed (throughput) for each link between each of the given M candidate APs and each of the given H hosts is assessed using the throughput estimation model in [31].
2. **Generation of Possible AP Combinations:** The total of ${}_M C_N$ possible combinations of N APs are generated by selecting N APs from the M candidates.
3. **Initialization of Objective Function:** The best-found objective functions E^{best} and E_2^{best} are initialized by 0, where E_2^{best} represents the best-found value of the average host throughput and E^{best} does the best-found value of the total bottleneck host throughput for N APs.
4. **Examination of New AP Combination:** For each combination of N APs, the following procedure is applied:
 - (a) The candidate AP that has the largest link speed is selected for the associated AP of each host.
 - (b) The best-found objective functions E^{best} and E_2^{best} are updated, and the current AP selection is saved in memory, if at least one of the two best found objective functions, E^{best} or E_2^{best} , is updated and another one remains the same by the current AP selection and the host associations.
5. **Termination check:** If every combination of N APs is examined, the procedure is terminated, and the selected N APs is used for the input to the active AP configuration algorithm. Otherwise, move to step (4) to analyze another new combination.

Fig. 9: Procedure of exhaustive search.

TABLE V: First extension simulation results for regular topology 2.

G mbps	Method	Min. h. throu.	Ave. Min. h throu.	Ave. h. throu.	Ave. Max. h. throu.	Total throu.
10	Original	0.04	0.23	0.58	0.79	17.54
	Only pre.	0.11	0.38	0.67	0.89	19.99
15	Original	0.51	1.01	2.73	4.08	82.19
	Only pre.	1.41	2.14	3.00	3.74	89.99
20	Original	0.67	1.86	4.47	6.15	134.23
	Only pre.	0.95	3.79	7.03	9.37	210.75
25	Original	1.05	3.59	8.04	12.26	241.45
	Only pre.	1.5	4.68	8.42	10.61	252.49
30	Original	2.41	7.11	10.58	13.85	317.64
	Only pre.	3.57	7.71	10.63	13.83	318.92

TABLE VI: Second extension simulation results for regular topology 2.

G mbps	Method	Min. h. throu.	Ave. Min. h throu.	Ave. h. throu.	Ave. Max. h. throu.	Total throu.
10	Original	0.04	0.23	0.58	0.79	17.54
	With pre. & post.	0.14	0.3	0.68	0.89	20.29
15	Original	0.51	1.01	2.73	4.08	82.19
	With pre. & post.	1.41	2.14	3.00	3.74	89.99
20	Original	0.67	1.86	4.47	6.15	134.23
	With pre. & post.	3.16	4.76	7.29	9.56	218.69
25	Original	1.05	3.59	8.04	12.26	241.45
	With pre. & post.	2.54	6.32	9.11	10.81	273.31
30	Original	2.41	7.11	10.58	13.85	317.64
	With pre. & post.	4.53	7.79	10.93	14.18	327.93

respectively. Figure 22 shows the number of active APs, CB or $non-CB$ POC for each AP, and the maximum or minimum transmission power for each AP for different value of G . Table V shows the minimum host throughput, the average minimum host throughput, the average host throughput, the average maximum host throughput, and the total throughput respectively. By considering the *pre-processing stage* in the first extension, the throughput performance is improved compared to the original method.

3) *Results of Second Extension:* Figure 23 and Table VI show the second extension results and the simulation results respectively. By considering both the *pre-processing* and *post-processing stages* in the second extension, the throughput performance is improved for all cases compared to the original method.

After implementing the second extension, significant throughput improvements are observed in most cases in Table VI when compared to the results from the first extension in Table V. To evaluate the effectiveness of the second extension, we compare the *pre-processing and post-processing* results for $G = 25$. Figure 24 depicts the regular network topology 2 with AP host associations for $G = 25$. In Figure

24 (a), only the pre-processing is considered, revealing that a few hosts experience poor associations, resulting in the lower throughput and the network performance degradation, indicated by the red marks. In Figure 24 (b), the second extension is illustrated, demonstrating improved associations through refining *AP-host associations*, which leads to overall improvements in the network performance.

E. First Extension Performance Analysis with Random AP Selection

In the first extension, we considered the *pre-processing stage*, where we mainly select the *promising candidate APs* depending on the network conditions. The first extension simulation results can be found in Tables I, III and V. These show that the results for random and regular topologies on the pre-processing stage of the AP joint optimization algorithm improve throughput performance compared to the original method. Furthermore, the pre-processing stage also reduced the *CPU* time by reducing the search space due to the selection of limited promising APs, which was already confirmed in [14].

If the promising APs are manually selected, gathering the

1. **Estimation of link speed:** The throughput of the link between each of M candidate APs and each of H hosts is calculated using the throughput estimation model [31].
2. **Initialization of associated AP for host:** The initial associated candidate AP is found for each host, and the non-associated candidate APs are excluded with four steps as below:
 - (a) Select the candidate AP for each host such that the throughput is maximized.
 - (b) Calculate the expected number of associated hosts per AP, n as follows:

$$n = AP_{max}/S \quad (1)$$
 Here, AP_{max} is the maximum throughput for each AP and S does the minimum required throughput for the association.
 - (c) For each candidate AP, sort all the hosts in descending order of the throughput with it. Then, for each candidate AP, select n hosts from the top of the sorted list, and calculate the total throughput of the links with the n hosts.
 - (d) Sort all the candidate APs in descending order of the total throughput in iii). From the top of the sorted AP list, select the candidate APs, until each host in the network is included in the set of hosts selected in iii) for the candidate APs selected in iv). The remaining candidate APs are excluded.
3. **Selection of removed candidate AP:** Find one candidate AP to be removed such that at least one of the two best found objective functions, E^{best} or E_2^{best} , can be updated, and another one remains the same after removing that AP for the current AP number.
 - (a) For each remaining candidate AP, discover the other remaining candidate AP to associate each associated host with this AP such that the throughput is maximized, and identify the minimum throughput (bottleneck host throughput) among the links to this AP after the host re-associations.
 - (b) Calculate the objective function E^{best} or E_2^{best} for the new associations.
 - (c) Remove the candidate AP if at least one of the two best found objective functions, E^{best} or E_2^{best} are becomes maximum and another one remains the same after applying i) and ii) to every remaining candidate AP, and apply the re-association for each associated host with this AP.
4. **Selection of N candidate APs:** Repeat Step 3 until the number of remaining candidate APs becomes N .

Fig. 10: Procedure of heuristic search.

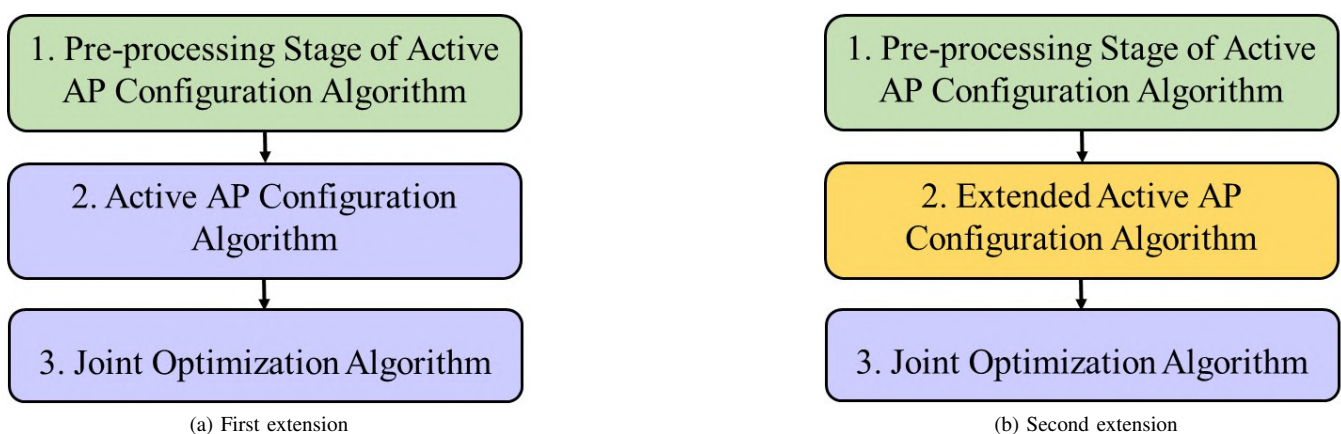


Fig. 11: Overall execution flow of the proposal.

necessary information takes a lot of effort and can be time-consuming. On the other hand, if they are randomly selected, it may carry the risk of poor selection. To evaluate the effectiveness of the pre-processing stage in the first extension, we compare the results with the results for randomly selecting

candidate APs. Figure 25 illustrates the overall execution flow for the joint optimization algorithm with the *random AP selection method*.

Figure 26 shows the network topology where candidate APs are selected randomly. Figure 26 (a) illustrates the

PC Model	Lenovo ThinkPad-L560
Processor	Inter(R), Core(TM) i3-6006U (2.00 GHz x 4)
Memory (RAM)	4 GB
OS	Ubuntu LTS 14.04, 64 bit
Simulator	WIMNET simulator [16]
Interface	IEEE 802.11n

Fig. 12: Simulation platform.

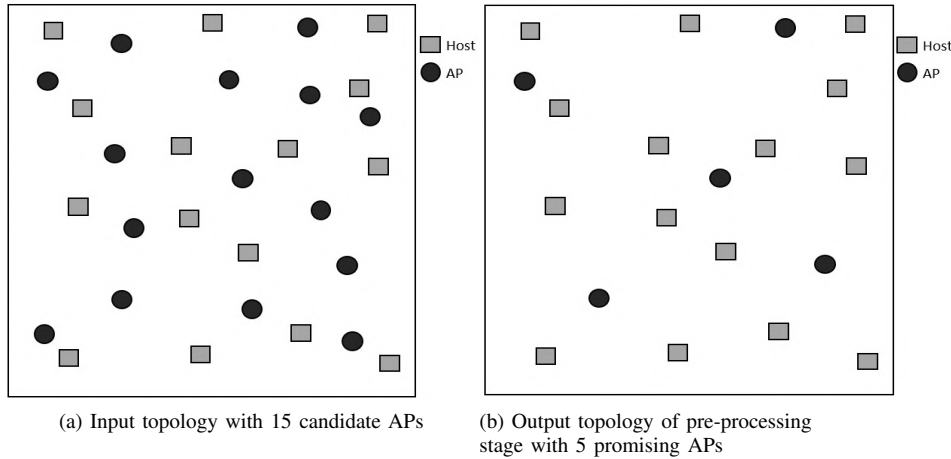


Fig. 13: Random topology.

G Mbps	No. of active APs (Orig./Prepro.)	Channel (Power) AP1, AP2, AP3, AP4, AP5	
		Original	Only preprocessing
10	2/2	1+5(max), 9+13(max)	9+13(max), 1+5 (max)
20	3/3	7(max), 13(max), 1(max)	1(max), 1+5(max), 9+13(max)
30	4/4	7(max), 13(max), 1(max), 1(max)	9+13(min), 1(min), 1+5(min), 13(min)
35	5/5	1+5(max), 13(min), 9+13(max), 9+13(max), 9+13(max)	13(min), 1+5(max), 1(min), 1+5(max), 9+13(min)

Fig. 14: Comparison of network configuration with first extension for random topology.

G mbps	No. of active APs (Orig./Pre. & post.)	Channel (Power) AP1, AP2, AP3, AP4, AP5	
		Original	With preprocessing & postprocessing
10	2/2	1+5 (max), 9+13(max)	1+5(max), 9+13 (max)
20	3/3	7(max), 13(max), 1(max)	1(max), 1+5(max), 9+13(max)
30	4/4	7(max), 13(max), 1(max), 1(max)	9+13(min), 1(min), 1+5(min), 13(min)
35	5/5	1+5(max), 13(min), 9+13(max), 9+13(max), 9+13(max)	13(min), 1+5(max), 1(min), 1+5(max), 9+13(min)

Fig. 15: Comparison of network configuration with second extension for random topology.

random topology with 5 randomly selected APs, Figure 26 (b) illustrates the regular topology 1 with 7 randomly selected APs, and Figure 26 (c) illustrates the regular topology 2 with 10 randomly selected APs.

Figure 27 shows the throughput comparison results between the random AP selection and the pre-processing methods for the random topology. Figures 27 (a) and 27 (b) describe the minimum host throughput, the average minimum host throughput, the average host throughput, and the total throughput, respectively. The simulation results demonstrate that the random AP selection method provides lower throughput performance compared to the pre-processing method for all the values of G . For $G = 35$, although the random AP selection method yields the slightly higher average minimum host throughput, the minimum host throughput and the

total throughput are lower than those of the *pre-processing method*.

Figure 28 shows the throughput comparison results between the random AP selection and the pre-processing methods for the regular topology 1. Figures 28 (a) and 28 (b) describe the minimum host throughput, the average minimum host throughput, the average host throughput, and the total throughput respectively. The simulations demonstrate that the random AP selection method yields the lower throughput performance than the pre-processing method for all the G values.

Figure 29 shows the throughput comparison results between the random AP selection and the pre-processing methods for the regular topology 2. Figures 29 (a) and 29 (b) describe the minimum host throughput, the average minimum

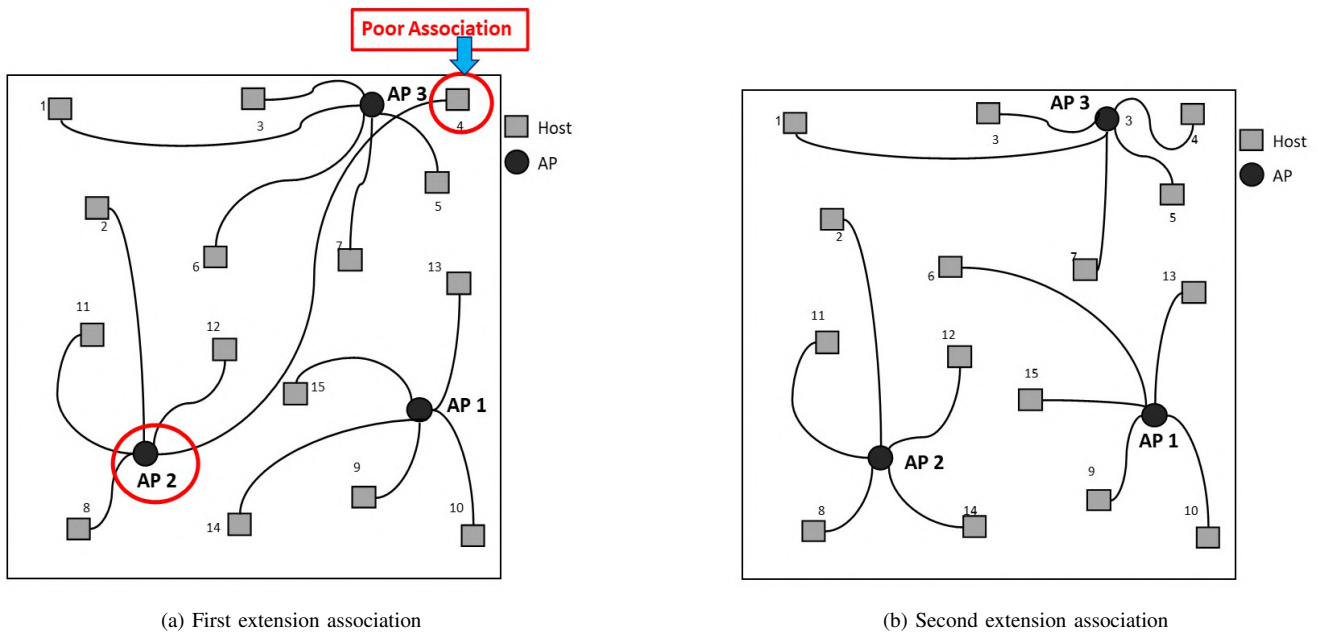


Fig. 16: AP host associations for G=20 in random topology.

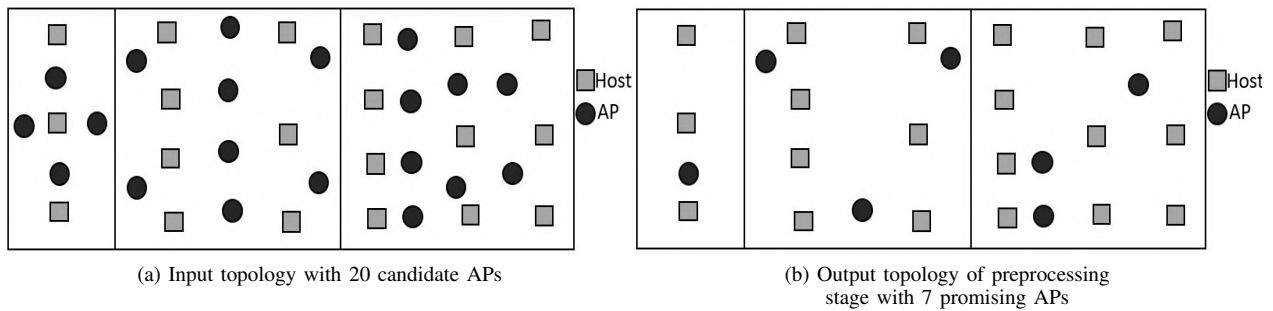


Fig. 17: Regular topology 1.

G Mbps	No. of active APs (Orig./Prepro.)	Channel (Power) AP1, AP2, AP3, AP4, AP5, AP6, AP7	
		Original	Only preprocessing
5	2/2	9+13(max), 1+5(max)	1+5(max), 9+13(max)
10	4/4	9+13(min), 1(max), 13(max), 7(max)	1+5(min), 13(max), 7(max), 1(max)
15	6/6	5+9(min), 13(min), 13(max), 13(max), 1(max), 7(max)	9+13(min), 1(max), 1(max), 9+13(min), 13(max), 1+5(min)
20	7/7	1(max), 13(min), 7(min), 13(min), 13(min), 9+13(min), 1+5(min)	1+5(min), 9+13(max), 9+13(min), 9+13(min), 1+5(min), 13(min), 9+13(max)

Fig. 18: Comparison of network configuration with first extension for regular topology 1.

host throughput, the average host throughput, and the total throughput respectively. The simulations demonstrate that the random AP selection method yields the lower throughput performance than the pre-processing method across all the G values. For G = 30, although the random AP selection method results in the slightly higher total throughput, the minimum host throughput and the average minimum host throughput are lower than those of the pre-processing method. The average host throughput is same for both methods.

From the above simulation results, we can see that for all the random and regular topologies, the random AP selection method yields the lower throughput performance compared to the pre-processing method. These results validate the

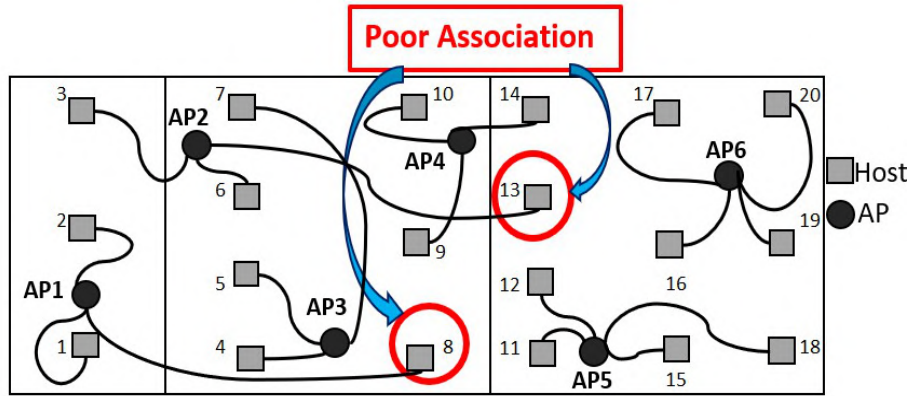
effectiveness of our first extension.

F. Greedy Approach Simulations Results

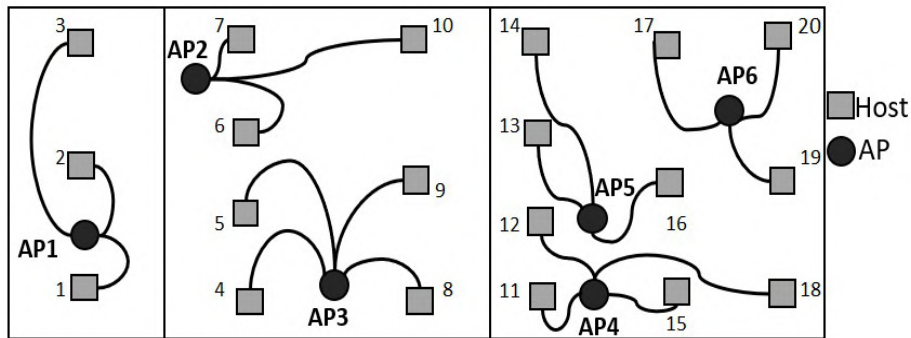
Tables VII, VIII, and IX show the simulation results for the greedy approach applied to random topology, regular topology 1, and regular topology 2, respectively. In the greedy approach, we assign the CB channel with maximum power to all active APs instead of joint optimization. However, the results indicate that this approach leads to worse throughput performance compared to the original method, as well as the first and second extensions.

G Mbps	No. of active APs (Orig./Pre. & post.)	Channel (Power)	
		AP1, AP2, AP3, AP4, AP5, AP6, AP7	
		Original	With preprocessing & postprocessing
5	2/2	9+13(max), 1+5(max)	1+5(max), 9+13(max)
10	4/4	9+13(min), 1(max), 13(max), 7(max)	1+5(min), 13(max), 7(max), 1(max)
15	6/6	5+9(min), 13(min), 13(max), 13(max), 1(max), 7(max)	9+13(min), 1(max), 1(max), 13(min), 9+13(min), 1+5 (min)
20	7/7	1(max), 13(min), 7(min), 13(min), 13(min), 9+13(min), 1+5(min)	9+13(min), 1+5(min), 1(min), 13(min), 1(max), 7(min), 1(max)

Fig. 19: Comparison of network configuration with second extension for regular topology 1.

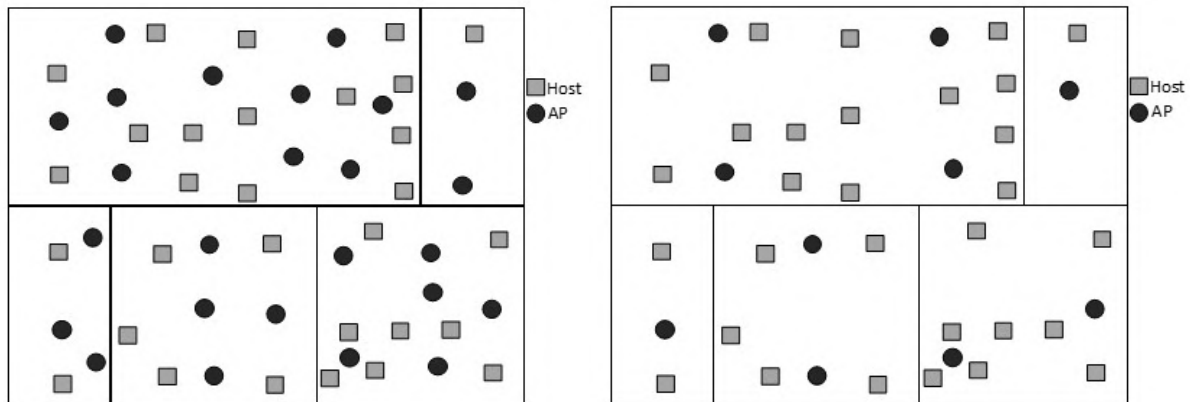


(a) First extension association



(b) Second extension association

Fig. 20: AP host associations for G=15 in regular topology 1.



(a) Input topology with 25 candidate APs

(b) Output topology of preprocessing stage with 10 promising APs

Fig. 21: Regular topology 2.

G Mbps	No. of active APs (Orig./Prepro.)	Channel (Power)	
		AP1, AP2, AP3, AP4, AP5, AP6, AP7, AP8	
		Original	Only preprocessing
10	3/3	1(min), 9+13 (max), 1+5(max)	9+13(max), 1+5(max), 1(max)
15	4/4	1+5(max), 9+13(min), 13(min), 1(max)	1(max), 1+5(max), 13(max), 9+13(max)
20	5/6	7(min), 1+5(min), 9+13(min), 13(max), 1(max)	1+5(max), 5+9(min), 1(min), 13(max), 9+13 (min), 1+5 (min)
25	7/7	13(max), 1(min), 5+9(min), 9+13(min), 1+5(min) , 13(min), 9+13(min)	9+13 (min), 13 (max), 1(max), 1+5(min), 1(max), 9+13(min), 5+9(min)
30	8/8	13(max), 13 (max), 1(max), 9+13(min), 1+5(min), 13 (max), 7(min), 1+5(min)	9+13 (min), 1 (max), 1 (min), 9+13(min), 9+13 (min), 1+5 (min), 1+5 (min), 13 (min)

Fig. 22: Comparison of network configuration with first extension for regular topology 2.

G Mbps	No. of active APs (Orig./Pre. & post.)	Channel (Power)	
		AP1, AP2, AP3, AP4, AP5, AP6, AP7, AP8	
		Original	With preprocessing & postprocessing
10	3/3	1(min), 9+13 (max), 1+5(max)	1+5(max), 9+13(max), 13(max)
15	4/4	1+5(max), 9+13(min), 13(min), 1(max)	1(max), 1+5(max), 13(max), 9+13(max)
20	5/6	7(min), 1+5(min), 9+13(min), 13(max), 1(max)	1+5(max), 5+9(min), 1(min), 13(max), 9+13(min), 1+5(min)
25	7/7	13(max), 1(min), 5+9(min), 9+13(min), 1+5(min) , 13(min), 9+13(min)	5+9(max), 13(max), 1(max), 7(max), 7 (min) , 1+5 (min), 9+13 (min)
30	8/8	13(max), 13 (max), 1(max), 9+13(min), 1+5(min), 13 (max), 7(min), 1+5(min)	9+13(min), 1(max), 1(min), 9+13(min), 9+13(min), 1+5(min), 1+5(min), 13(min)

Fig. 23: Comparison of network configuration with second extension for regular topology 2.

TABLE VII: Greedy approach simulation results for random topology.

G mbps	Min. h. throu.	Ave. Min. h throu.	Ave. h. throu.	Ave. Max. h. throu.	Total throu.
10	2.27	2.59	3.39	4.09	50.87
20	2.85	3.33	4.21	4.93	63.23
30	3.11	4.97	5.7	6.28	85.52
35	5.28	6.22	7	7.75	105.01

TABLE VIII: Greedy approach simulation results for regular topology 1.

G mbps	Min. h. throu.	Ave. Min. h throu.	Ave. h. throu.	Ave. Max. h. throu.	Total throu.
5	0.69	0.82	1.07	1.25	21.52
10	3.24	4.16	4.69	5.17	93.9
15	3.96	5.02	6.01	6.81	120.17
20	5.88	7.67	7.69	8.16	153.98

TABLE IX: Greedy approach simulation results for regular topology 2.

G mbps	Min. h. throu.	Ave. Min. h throu.	Ave. h. throu.	Ave. Max. h. throu.	Total throu.
10	0.11	0.22	0.44	0.55	13.13
15	0.59	0.92	1.71	2.17	51.23
20	0.69	1.54	2.46	2.91	73.83
25	1.27	3.07	4.69	5.63	140.84
30	3.36	4.8	6.09	7.39	182.8

G. Discussions of Simulations Results

Tables X, XI, and XII show the throughput performance for random topology, regular topology 1, and regular topology 2, respectively. The results demonstrate that the second extension results are better than the original, greedy, and

first extension, which proves the validity of the proposal. The results of the first extension improvement show that the pre-processing stage enhances the solution quality by optimizing the promising active APs compared to the original and greedy method. Additionally, the results of the second extension demonstrate that the post-processing stage has an impact on the host association and improves the throughput performance, which is better than the original, greedy method and the first extension. These results highlight the superior throughput performance of our proposal.

VII. CONCLUSION

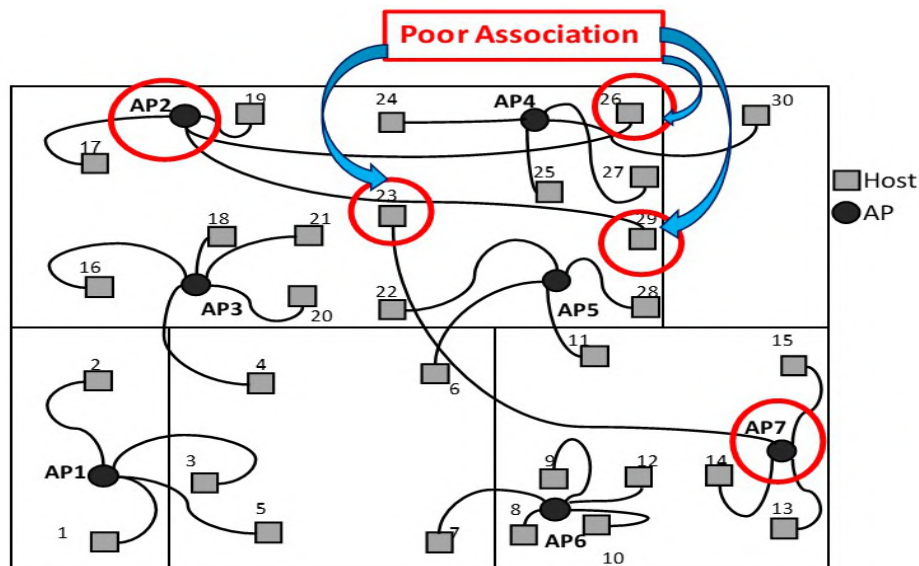
This paper presented the two extensions of the AP joint optimization algorithm. In the first extension, we considered the *pre-processing stage* of the active AP configuration algorithm that identify promising candidate APs from a broad number of APs. In the second extension, we presented the *post-processing stage* that refines the AP-host associations and considered the use of both stages in the AP joint optimization algorithm. We demonstrated our proposal validity through simulations utilizing the WIMNET simulator. The results confirmed that the proposal improved the throughput performance by reducing the interference level compared to the original methods. In future work, we will evaluate our proposal in a variety of network fields and compare it with other metrics and schemes in different fields to assess its effectiveness.

APPENDIX A

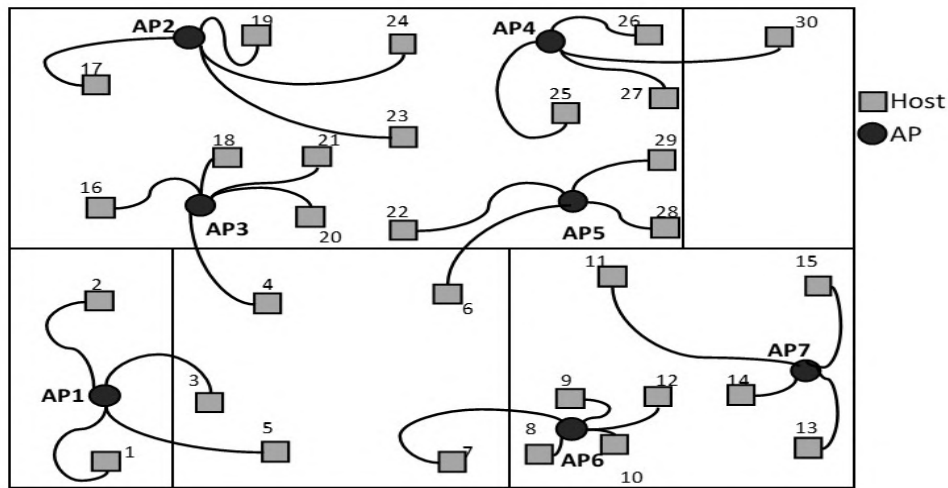
THROUGHPUT DROP ESTIMATION MODEL

The *channel*, *physical*, and the *link distance* are described in Figure 30 .

Figures 31 describes the model under non-interference.



(a) First extension association



(b) Second extension association

Fig. 24: AP host associations for G=25 in regular topology 2.

TABLE X: Throughput performance of random topology.

Results	Method	Min. host	Ave. min. host	Ave. host	Max. host	Ave. max. host	Total
Throu. (Mbps.)	Original	13.8	23.72	30.56	54.88	36.05	450.46
	Greedy	13.51	17.11	20.3	29.71	23.05	304.63
	Only pre.	18.3	27.31	33.48	63.3	39.14	502.11
	With pre. & post.	18.37	28.3	34.91	63.19	39.16	509.48
Improvement with original (%)	Only pre.	32.61	15.13	9.55	15.34	8.578	11.46
	With pre. & post.	33.11	19.31	14.23	15.14	8.62	13.10
Improvement with greedy (%)	Only pre.	35.45	59.61	64.92	113.03	69.81	64.82
	With pre. & post.	35.97	65.40	71.97	112.66	69.89	67.24

Figures 32 describes the model for interfered link under CB.

Figures 33 describes the model for interfered link under non-CB.

Figures 34 describes the model under coexistence of CB and non-CB links.

REFERENCES

- [1] B. P. Crow, I. Widjaja, J. G. Kim, and P. T. Sakai, "IEEE 802.11 wireless local area networks," *IEEE Commun. Mag.*, vol. 35, no. 9, pp. 116-126, Sept. 1997.
- [2] M. Balazinska and P. Castro, "Characterizing mobility and network usage in a corporate wireless local-area network," *Proc. Int. Conf. Mobile Systems, Appl. Services*, pp. 303-316, 2003.
- [3] S. Zeadally, O. Bello, "Harnessing the power of Internet of Things based connectivity to improve healthcare," *Int. Things (2019) 100074*.
- [4] H.A. El Zouka, M.M. Hosni, "Secure IoT communications for smart healthcare monitoring system," *Int. Things (2019) 100036*.

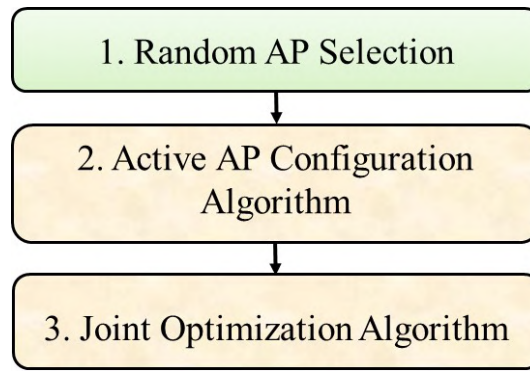


Fig. 25: Flow of joint optimization algorithm with random AP selection method.

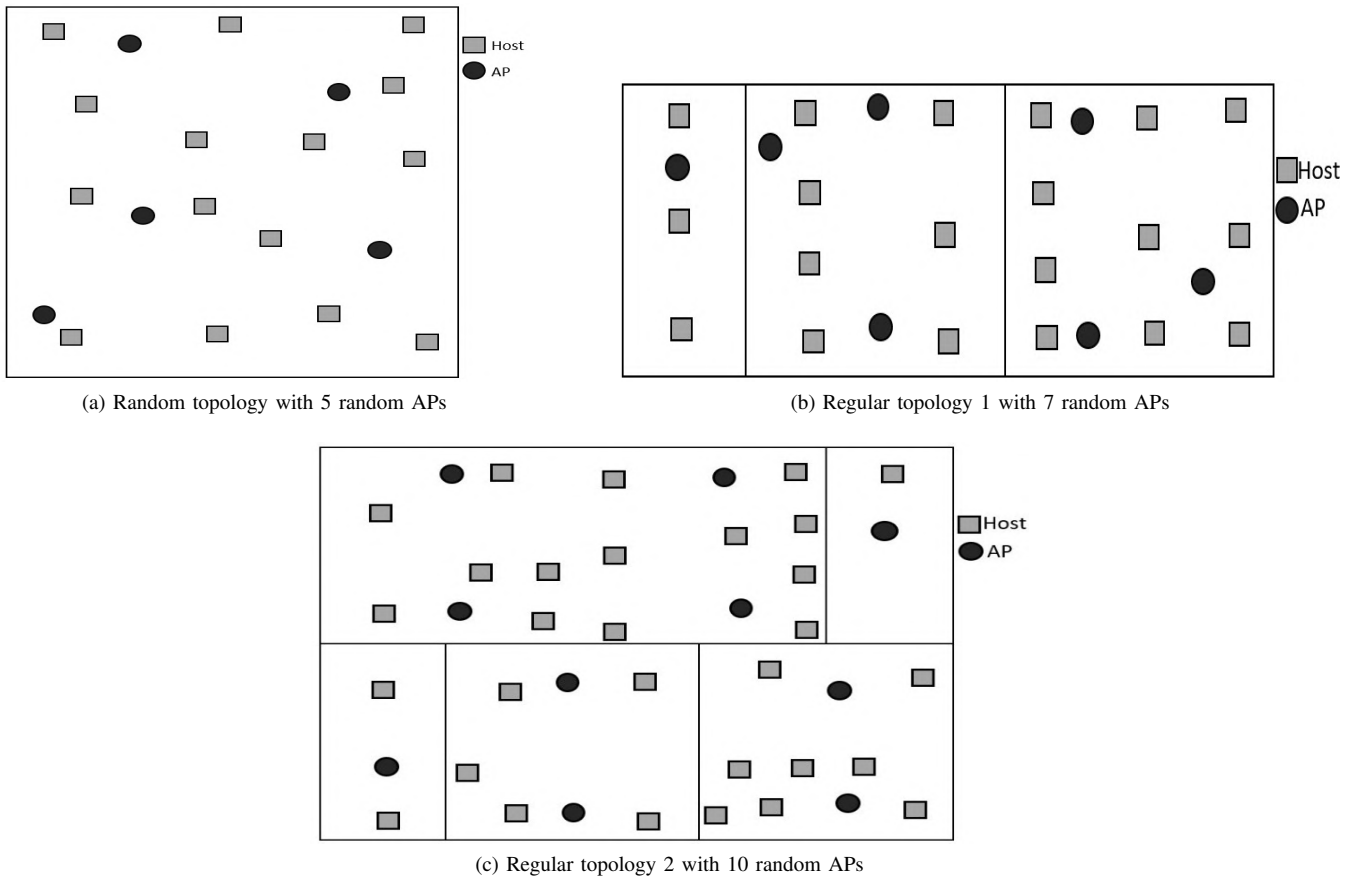


Fig. 26: Topologies for random AP selection method.

TABLE XI: Throughput performance of regular topology 1.

Results	Method	Min. host	Ave. min. host	Ave. host	Max. host	Ave. max. host	Total
Throu. (Mbps.)	Original	12.50	25.42	31.41	55.05	36.68	628.52
	Greedy	13.77	17.67	19.46	28.81	21.39	389.57
	Only pre.	16.98	32.32	36.24	80.41	42.68	725.17
	With pre. & post.	18.35	30.80	37.00	81.78	43.88	740.25
Improvement with original (%)	Only pre.	35.84	27.14	15.37	46.06	16.35	15.37
	With pre. & post.	46.8	21.16	17.79	48.55	19.62	17.77
Improvement with greedy (%)	Only pre.	23.31	82.91	86.22	179.11	99.53	86.14
	With pre. & post.	33.26	74.31	90.13	183.85	105.14	90.01

[5] D. Mocrii, Y. Chen, P. Musilek, "IoT-based smart homes: A review of system architecture, Software, Communications, Privacy and Security," *Int. Things 1 (2018) 81-98*.

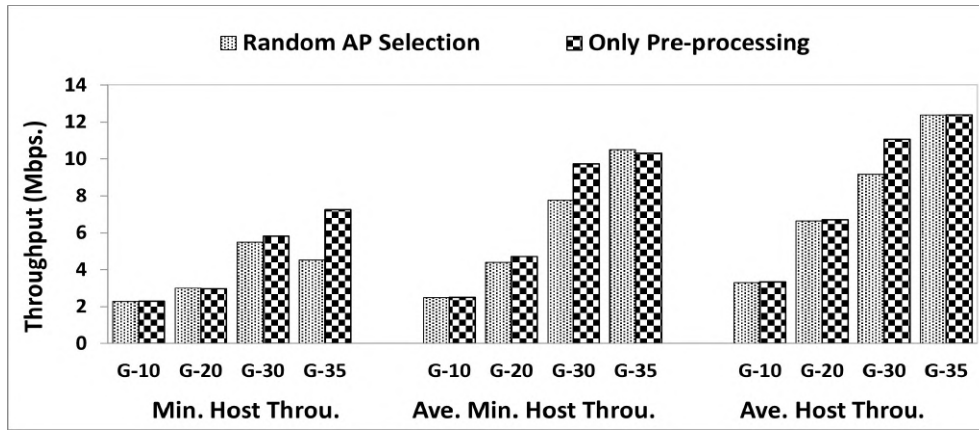
[6] M. M. Islam, N. Funabiki, R. W. Sudibyo, K. I. Munene, W. C. Kao, "A dynamic access-point transmission power minimization method using PI feedback control in elastic WLAN system for IoT applications," *Int. Things 8 (2019) 100089*.

[7] J. O. Agyemang, J. J. Kponyo, G. S. Klogo, J. O. Boateng, "Lightweight rogue access point detection algorithm for WiFi-enabled internet of things (IoT) devices," *Int. Things 11 (2020) 100200*.

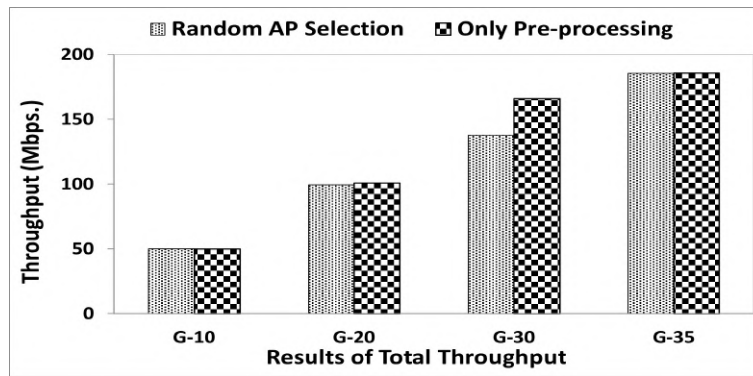
[8] J. Talvitie, M. Renfors, E.S. Lohan, "A comparison of received signal strength statistics between 2.4 GHz and 5 GHz bands for WLAN-based indoor positioning," in: *Proc. Globecom Work. 2015*, pp. 1-6.

[9] National Instrument, Introduction to wireless LAN measurements from 802.11a to 802.11ac, 2018.

[10] S. Lanzisera, B. Nordman, and R. E. Brown, "Data network equipment

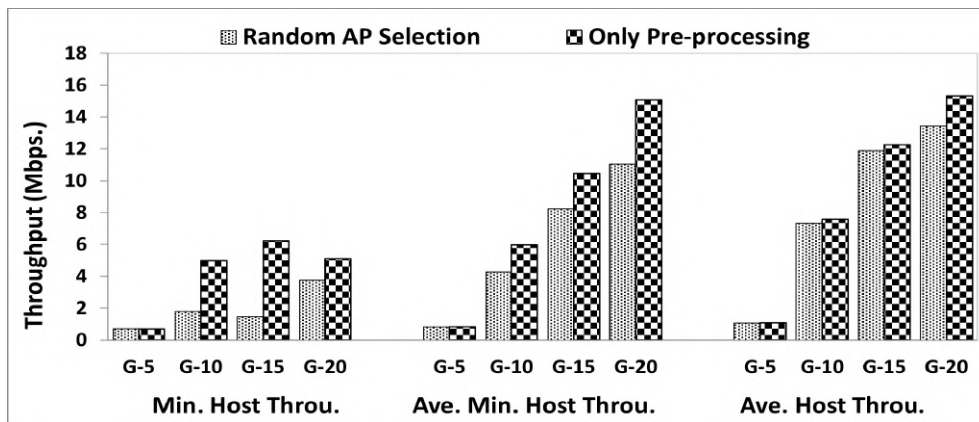


(a) Min. host, ave. min. host, and ave. host throughput

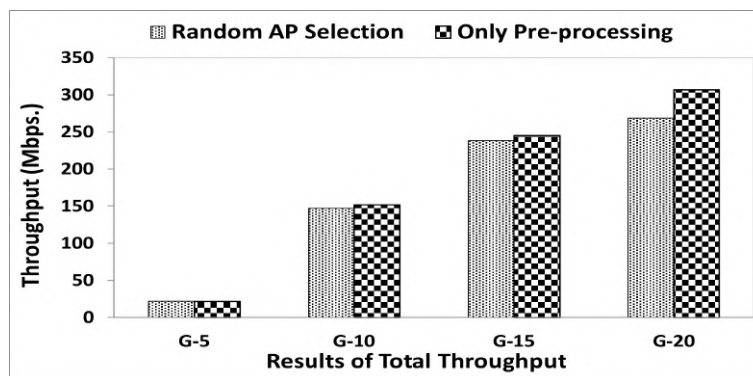


(b) Total throughput

Fig. 27: Throughput comparison between random AP selection and pre-processing methods for random topology.

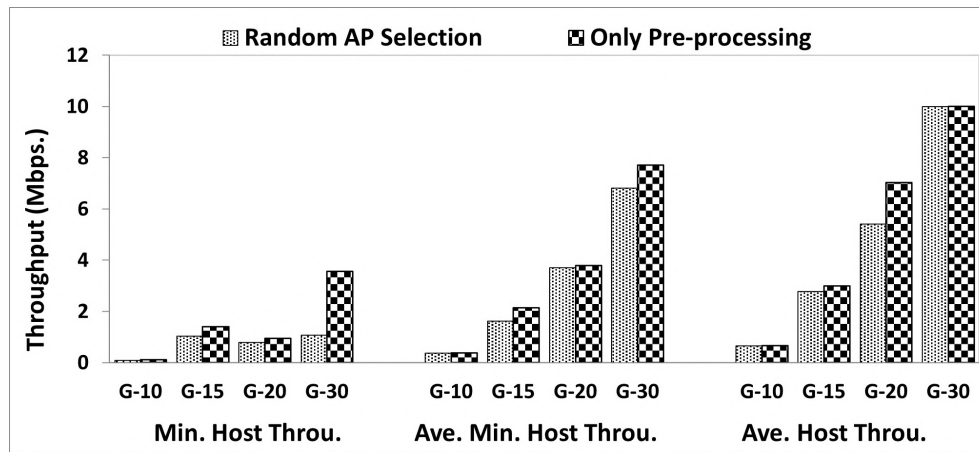


(a) Min. host, ave. min. host, and ave. host throughput

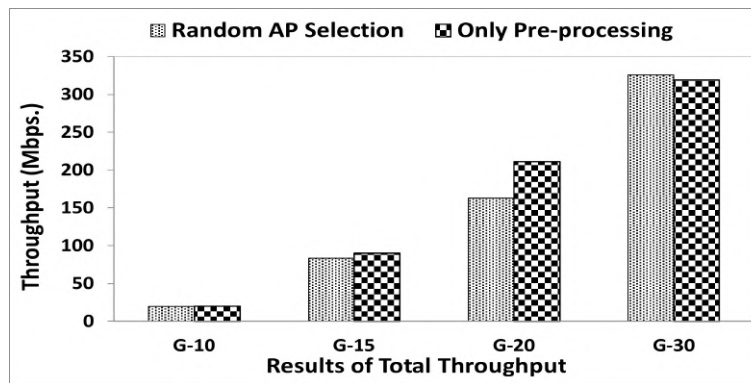


(b) Total throughput

Fig. 28: Throughput comparison between random AP selection and pre-processing methods for regular topology 1.



(a) Min. host, ave. min. host, and ave. host throughput



(b) Total throughput

Fig. 29: Throughput comparison between random AP selection and pre-processing methods for regular topology 2.

TABLE XII: Throughput performance of regular topology 2.

Results	Method	Min. host	Ave. min. host	Ave. host	Max. host	Ave. max. host	Total
Throu. (Mbps.)	Original	4.68	13.8	26.4	57.71	37.13	793.05
	Greedy	6.02	10.55	15.39	25.24	18.65	461.83
	Only pre.	7.54	18.7	29.75	57.81	38.44	892.14
	With pre. & post.	11.78	21.31	31.01	63.77	39.18	930.21
Improvement with original (%)	Only pre.	61.11	35.51	12.68	0.17	3.52	12.49
	With pre. & post.	151.71	54.42	17.46	10.51	5.52	17.29
Improvement with greedy (%)	Only pre.	25.24	77.25	93.31	129.02	106.11	93.17
	With pre. & post.	95.68	101.99	101.49	152.63	110.08	101.42

Definitions of Three Distances in Throughput Estimation Model

The *channel distance*, the *physical distance*, and the *link distance* are described here.

1. *Channel distance (chD)* describes the minimum channel difference between the channels of the two links. For example, when both links are assigned the same channel, *chD* is 0, where they will be fully overlapped. On the other hand, when one link is assigned *channel 1* and another link *channel 3*, *chD* is 2.
2. *Physical distance (phD)* describes the Euclidean distance between the two APs of the links. By expanding the *phD* between the links, the interfered signal declines due to the path loss and the absorption by obstacles.
3. *Link distance (lkD)* describes the Euclidean distance between the transmitter and receiver of the link. Since the signal is propagated from the transmitter to the receiver, the longer *lkD* reduces the *RSS* at the receiver and can degrade the throughput.

Fig. 30: Definition of three distances.

energy use and savings potential in buildings,” *Energy Efficiency*, vol. 5, no. 2, pp. 149-162, May 2012.

[11] K. Mittal, E. M. Belding, and S. Suri, “A game-theoretic analysis of wireless access point selection by mobile users,” *Computer Commun.*,

vol. 31, no. 10, pp. 2049-2062, Jan. 2008.

[12] M. S. A. Mamun, M. E. Islam, and N. Funabiki, “An active access-point configuration algorithm for elastic wireless local-area network system using heterogeneous devices,” *Int. J. Netw. Comput.*, vol. 6,

Throughput Estimation Model under Non-Interference

In [31], exhibited the *throughput estimation model* for a single link under no interference. This model estimates the *receiving signal strength (RSS)* at the host applying the *log distance path loss model* [34]:

The Euclidean distance $d(m)$ is estimated for each link (AP/host pair) by:

$$d = \sqrt{(AP_x - H_x)^2 + (AP_y - H_y)^2} \quad (1)$$

where AP_x, AP_y and H_x, H_y does the x and y coordinates for the AP and the host respectively.

Then, $d(m)$ is used to calculate RSS_d in Eq. (2) by:

$$RSS_d = P_1 - 10\alpha \log_{10} d - \sum_k n_k W_k \quad (2)$$

where RSS_d describes RSS ($-dBm$) at the host, P_1 does RSS at $1m$ distance from the AP when no obstacle exists, α does the path loss exponent, $d(m)$ does the Euclidean distance between the AP and the host, n_k does the number of *type-k* obstacles along the path from the AP to the host, and W_k does the signal attenuation factor (dBm) for *type-k* obstacle. The parameters P_1, α , and W_k are obtained by running our parameter optimization tool [35] with the measurement data.

Next, this model converts RSS_d to the estimated throughput tp_{ij} utilizing the *sigmoid function*:

$$tp_{ij} = \frac{a}{1 + e^{-\left(\frac{120 + RSS_d}{c} - b\right)}} \quad (3)$$

where tp_{ij} describes the estimated throughput ($Mbps$) and a, b , and c are constant coefficients whose values were obtained by executing our parameter optimization tool [35] with the measurement data.

Fig. 31: Model for non-interference.

- no. 2, pp. 395-419, July 2016.
- [13] M. S. A. Mamun, N. Funabiki, K. S. Lwin, M. E. Islam, and W.-C. Kao, "A channel assignment extension of active access-point configuration algorithm for elastic WLAN system and its implementation using Raspberry Pi," *Int. J. Netw. Comput.*, vol. 7, no. 2, pp. 248-270, July, 2017.
- [14] M. Saha, N. Funabiki, S. K. Debnath, W.-C. Kao, S. Tajima, and T. Higashino, "A proposal of preprocessing stage for active access point configuration algorithm in elastic WLAN system," *ICIET*, pp. 284-289, March 28-30, 2020.
- [15] K. I. Munene, N. Funabiki, M. M. Rahman, H. Briantor, S. C. Roy, and M. Kuribayashi, "A throughput drop estimation model and its application to joint optimization of transmission power, frequency channel, and channel bonding in IEEE 802.11n WLAN for large-scale IoT Environments," *Int. Things 20 (2022) 100583*.
- [16] N. Funabiki, ed., "Wireless mesh networks," InTech-Open Access Pub., Jan. 2011, <http://www.intechopen.com/books/wireless-mesh-networks>, *Access Jan. 20, 2017.Int. Works. Virtual Environ. Net. -Ori. Appli. (VENOA-2017)*, pp. 701-710, July 2017.
- [17] H. U. Lee, W. S. Jeon, and D. G. Jeong, "An effective AP placement scheme for reliable WiFi connection in industrial environment," *Asso. for Comp. Mach.*, pp. 2137-2143, April 2020.
- [18] S. B. A. Khattak, M. M. Nasralla, M. Marey, M. A. Esmail, M. Jia and M. Y. Umair, "WLAN access points channel assignment strategy for indoor localization systems in smart sustainable cities," *IOP Conf. Series: Ear. and Env. Sci. (ICSDI)*, 2022.
- [19] R.G. Garroppo, G. Nencioni, L. Tavanti, B. Gendron, M.G. Scutell, "Optimal access point power management for green IEEE 802.11 networks," *Sensors* 2021.
- [20] L. M. Ali and O. Khanji, "Location-allocation optimization of Wi-Fi access points at Gaziantep University campus," in *Proce. Int. Conf. Indus. Eng. Ope. Manag. Manila*, pp. 2125-2136, March 2023.
- [21] P. Liu, X. Meng, J. Wu, M. Yao, Z. Tang, "AP deployment optimization for WLAN: a fruit fly optimization approach," in *Proc. Int. Conf. Comm. China (ICCC)*, pp. 478-483, 2019.
- [22] S. C. Roy, N. Funabiki, M. M. Rahman, B. Wu, M. Kuribayashi, and W. C. Kao, "A study of the active access-point configuration algorithm under channel bonding to dual IEEE 802.11n and 11ac interfaces in an elastic WLAN system for IoT applications," *Signals*, vol. 4, pp. 274-296, 2023.
- [23] B. P. Tewari and S. C. Ghosh, "Combined power control and partially overlapping channel assignment for interference mitigation in dense WLAN," *In Proceedings of AINA*, pages 646-653, 2017.
- [24] A. Kachroo, J. Park, H. Kim, "Channel assignment with transmission power optimization method for high throughput in multi-access point WLAN," in: *Proc. Wire. Commu. Mob. Comp. Conf. 2015*, pp. 314-319.
- [25] H. Shindo, T. Nagai, and H. Shigeno, "Virtual access point allocation method for high density WLANs," in *Proc. Int. Conf. Mob. Comput. Ubi. Network.*, pp. 69-76, 2012.
- [26] X. Yang, B. Chen, and F. Gao, "How to select measurement points in access point localization," *Lecture Notes in Engineering and Computer Science: Proceedings of the International MultiConference of Engineers and Computer Scientists 2015*, Vol II, IMECS 2015, 18-20 March, 2015, Hong Kong, pp 571-576.
- [27] Y. Kobayashi, J. Takahashi, and Y. Tobe, "A mobile Wi-Fi access point considering types and volumes of traffic," *Lecture Notes in Engineering and Computer Science: Proceedings of the World Congress on Engineering 2017*, Vol I, WCE 2017, 5-7 July, 2017, London, U.K., pp 519-523.
- [28] M. Alakhras, M. Oussalah, and M. Hussein, "Resource allocation model based on interval for wireless network with guaranteed QoS," *Lecture Notes in Engineering and Computer Science: Proceedings of the World Congress on Engineering 2018*, Vol I, WCE 2018, 4-6 July, 2018, London, U.K., pp 399-402.
- [29] P. Mestre, A. Fonseca, P. Salgado, and C. Serodio, "WiFi access point selector based on the network delay," *Lecture Notes in Engineering and Computer Science: Proceedings of the World Congress on Engineering 2018*, Vol I, WCE 2018, 4-6 July, 2018, London, U.K., pp 409-414.
- [30] C. Deng, and N. Li, "Optimization of the layout of WLAN access point based on location reliability," *Lecture Notes in Engineering and Computer Science: Proceedings of the International MultiConference of Engineers and Computer Scientists 2017*, Vol II, IMECS 2017, 15-17 March, 2017, Hong Kong, pp 604-607.
- [31] K. S. Lwin, N. Funabiki, C. Taniguchi, K. K. Zaw, M. S. A. Mamun, M. Kuribayashi, W.-C. Kao, "A minimax approach for access point setup optimization in IEEE 802.11n wireless networks," *Int. J. Netw. Comp.*, vol. 7, no. 2, pp. 187-207, 2017.
- [32] L. A. Wolsey, "An analysis of the greedy algorithm for the submodular set covering problem," *Combinatorica*, vol. 2, no. 4, pp. 385-393, Dec. 1982.
- [33] D. P. Williamson and D. B. Shmoys, "The design of approximation algorithms," *Cambridge Univ. Press*, Apr. 2011.

Throughput Drop Model for Interfered Link under CB

In [36, 37], exhibited the *throughput drop estimation model* under interfered *CB* links. For two interfered links, this model adopts the *logarithm function* of the RSS, RSS^i and the *chD* from the interfered link in Eq. (4).

$$tpD(RSS^i, chD) = p(chD) \times \ln(q(chD) + RSS^i) + r(chD) \quad (4)$$

where $tpD(RSS^i, chD)$ describes the estimated throughput drop (*Mbps*), and $p(chD)$, $q(chD)$, and $r(chD)$ describe the constants determined by the channel distance (*chD*). The *physical distance* (*phD*) between the two APs is closely related with the RSS (RSS^i) of the interfered signal at the AP. When *phD* increases, the corresponding RSS^i decreases, as shown in Eq. (2) where RSS_d represents RSS^i and d does *phD*. The values of the three constant parameters in Eq. (4), p , q , and r , in [36] are computed from the throughput drop measurement results for each *chD* by running *Origin Pro8* software [38].

The interfered link causing the highest drop is considered first. Then, the interfered link causing the second highest drop is considered, which further reduces the throughput by increasing the contention. The following procedure is executed:

1. Calculate the throughput of the target link using the model under non-interference.
2. Calculate the throughput drop tpD from each interfered link using Eq. (4).
3. Sort the links in descending order of the drop magnitude. Here, the two interfered links are considered to the target link, where the drops are given by tpD^{1st} and tpD^{2nd} .
4. For the largest interfered link, adjust tpD^{1st} by the maximum speed of the AP of the target link, because the different APs may have the different throughput performances. The largest interfered link is defined as the interfered link that causes the largest throughput drop (tpD) at the target link.

$$tpD_{adj}^{1st} = tpD^{1st} \times \frac{tpM^{AP}}{140} \quad (5)$$

where tpD_{adj}^{1st} describes the adjusted throughput drop by the largest interfered link, tpM^{AP} does the maximum throughput for the AP of the target link, and 140 does the maximum throughput (*Mbps*) under channel bonding (*CB*) for *NEC AP* adopted in the model.

Then, the throughput tp_{ij}^{1st} of the target link is calculated after considering the drop by the first interfered link by:

$$tp_{ij}^{1st} = tp_{ij} - tpD_{adj}^{1st}. \quad (6)$$

5. For the second interfered link, adjust the tpD^{2nd} by:

$$tpD_{adj}^{2nd} = tpD^{2nd} \times \frac{tpM^{AP} - tpD_{adj}^{1st}}{140}. \quad (7)$$

The throughput tp_{ij}^{2nd} of target link is calculated after considering the drop by the second interfered link by:

$$tp_{ij}^{2nd} = tp_{ij}^{1st} - tpD_{adj}^{2nd}. \quad (8)$$

6. If more interfered links exist, repeat the same procedure.

The throughput drop's actual value depends on the device's throughput range at the target link. Eq. (4) was introduced to estimate the throughput drop, where the maximum link-speed of the target link is 140 *Mbps* for the *NEC WG2600HP* AP device with *CB* used in the experiments. For other devices whose maximum speed is different from 140 *Mbps*, this value needs to be adjusted linearly by its maximum speed, as confirmed by experiments.

Fig. 32: Model for *CB*.

[34] D. B. Faria, "Modeling Signal Attenuation in IEEE 802.11 Wireless LANs," *Tech. Report, TRKP06-0118, Stanford Univ*, 2005.

[35] N. Funabiki, C. Taniguchi, K.S. Lwin, K.K. Zaw, W.-C. Kao, "A parameter optimization tool and its application to throughput estimation model for wireless LAN," in: *Proc. Int. Work. Virtual Environ. Netw.-Orient. Appli.* 2017, pp. 701-710.

[36] K. I. Munene, N. Funabiki, M. M. Islam, M. Kuribayashi, M. S. A. Mamun, R. W. Sudibyo, and W.-C. Kao, "An extension of throughput drop estimation model for three-link concurrent communications under partially overlapping channels and channel bonding in IEEE 802.11n WLAN," *Adv. Sci. Technol. Eng. Syst. J.*, vol. 4, no. 4, pp. 94-105, 2019.

Throughput Drop Model for Interfered Link under non-CB

In [39], exhibited the *throughput drop estimation model* under interfered *non-CB* links. According to the measurement results, the *natural logarithm function* in Eq. (4) is again used to estimate the *throughput drop* (tpD) for *non-CB* links. The parameter values are tuned from measurement results of each chD [15].

For three or more interfered links, the interfered links are explored sequentially in descending order of their throughput drops as for *CB* links. First, the throughput drop in Eq. (5) and Eq. (7) is adjusted to consider the difference of the maximum throughput of the APs for *non-CB* (75Mbps) and *CB* (140Mbps) as follows:

$$tpD_{adj}^{1st} = tpD^{1st} \times \frac{tpM^{AP}}{75} \quad (9)$$

$$tpD_{adj}^{2nd} = tpD^{2nd} \times \frac{tpM^{AP} - tpD_{adj}^{1st}}{75} \quad (10)$$

Then, the dropped throughput under the interferences for the target link is obtained by sequentially subtracting the tpD_{adj}^{1st} and tpD_{adj}^{2nd} from tp_{ij} , as in Eq. (6) and Eq. (8).

Fig. 33: Model for non-CB.

Throughput Drop Model under Coexistence of CB and non-CB Links

In [15], exhibited throughput drop measurements under coexistence of *CB* and *non-CB* links.

According to the throughput drop measurement results, in [15] calculated the *throughput drop* (tpD) from the interfered *received signal strength* (RSS^i) and the *channel distance* (chD), as in Eq. (4). The parameter values are tuned from measurement results under coexistence of *CB* and *non-CB* as in [15] by running *Origin Pro8* software.

Again for the multiple interfered links, the interfered links are explored sequentially in descending order of their throughput drops. Here only two interfered links are described.

1. When both of the interfering APs adopt *CB*, calculate the throughput drop under *CB* in [37].
2. When both of the interfering APs adopt *non-CB*, calculate the throughput drop under *non-CB* in [39].
3. When one AP adopts *CB* and another does *non-CB*, the following procedure is applied:
 - (a) Calculate the single link throughput for each host by Eq. (2) and Eq. (3).
 - (b) Calculate the sum of the throughput drops for the two APs by Eq. (4) utilizing the parameters in [15].
 - (c) Sort the links in descending order of the throughput drops that are given by tpD^{1st} and tpD^{2nd} .
 - (d) For the largest interfered link, adjust tpD^{1st} with the maximum speed of the target AP by Eq. (11) and Eq. (12).

$$tpD_{adj}^{1st} = tpD^{1st} \times \beta \times \frac{tpM^{AP}}{140}. \quad (11)$$

$$tpD_{adj}^{1st} = tpD^{1st} \times \beta \times \frac{tpM^{AP}}{75}. \quad (12)$$

It is assumed that one AP represents the target AP and the other does interfering AP. Eq. (11) is applied if the target AP uses *CB*, and Eq. (12) is applied otherwise. β represents the throughput drop normalization factor of 0.635 for *CB* and 0.365 for *non-CB*.

- (e) For the second interfered link, adjust the tpD^{2nd} by Eq. (13) and Eq. (14) for the target AP with *CB* and the AP with *non-CB* respectively.

$$tpD_{adj}^{2nd} = tpD^{2nd} \times \beta \times \frac{tpM^{AP} - tpD_{adj}^{1st}}{140}. \quad (13)$$

$$tpD_{adj}^{2nd} = tpD^{2nd} \times \beta \times \frac{tpM^{AP} - tpD_{adj}^{1st}}{75}. \quad (14)$$

Then, the dropped throughput under the interferences for the target link is obtained by sequentially subtracting tpD_{adj}^{1st} and tpD_{adj}^{2nd} from tp_{ij} , as in Eq. (6) and Eq. (8).

- (f) If more interfered links exist, repeat the same procedure.

Fig. 34: Model for both CB and non-CB.

- [37] I. M. Kwenga, N. Funabiki, M. M. Islam, M. Kuribayashi, R. W. Sudibyo, and W. -C. Kao, "A throughput estimation model under two-link concurrent communications with partially overlapping channels and its application to channel assignment in IEEE 802.11n WLAN," *Int. J. Space-Base. Situ. Comp.*, vol. 8, no. 3, pp. 123-137, 2018.
- [38] OriginLab [online], "<https://www.originlab.com/>" (accessed: 25 June 2023).
- [39] K. I. Munene, N. Funabiki, H. Briantoro, M. M. Rahman, F. Akhter, M. Kuribayashi, and W. -C. Kao, "A throughput drop estimation model for concurrent communications under partially overlapping channels without channel bonding and its application to channel assignment in IEEE 802.11n WLAN," *IEICE Trans. Inform. Syst.*, vol. E104-D, no. 5, pp. 585-596, May, 2021.

Mousumi Saha received B.S. degree in Telecommunication and Electronic Engineering from Hajee Mohammad Danesh Science and Technology University, Bangladesh, in 2013. She completed her master degree in Graduate School of Natural Science and Technology from Okayama University, Japan, in 2019. She is currently a Ph.D. student in Graduate School of Natural Science and Technology at Okayama University, Japan. Her research interest includes wireless communication and networking.

Nobuo Funabiki received B.S. and Ph.D. degrees in Mathematical Engineering and Information Physics from the University of Tokyo, Japan, in 1984 and 1993, and M.S. in Electrical Engineering from Case Western Reserve University, USA, in 1991. Since 2001, he has been a professor in Graduate School of Natural Science and Technology, Okayama University, Japan. His research interests include computer network, optimization algorithm, and educational technology. He is a member of IEEE, IEICE, and IPSJ.

Bin Wu received B.S. degree in Electronic Information Engineering from North China Electric Power University, China, in 2021. He is currently a postgraduate student in Graduate School of Natural Science and Technology at Okayama University, Japan. His areas of research focus on wireless communication and networking.

Pradini Puspitaningayu received B.E. degree in Electrical Engineering from Brawijaya University (Malang, Indonesia) in 2010 and M.E. in Telecommunication & Multimedia from Institut Teknologi Sepuluh Nopember (Surabaya, Indonesia) in 2014. She received Ph.D. degree in Graduate School of Natural Science and Technology at Okayama University, Japan, in 2022. From 2010-2012 she was with Samsung Electronics Indonesia, Ltd. as R&D engineer. She has been a lecturer in Universitas Negeri Surabaya, Indonesia since 2014. Her research interest includes positioning, wireless communication and networking.